Balanced estimate and uncertainty assessment of European climate change using the large EURO-CORDEX regional climate model ensemble

Guillaume Evin[1], Samuel Somot[2], and Benoit Hingray[3]

[1]Univ. Grenoble Alpes, INRAE, UR ETGR, Grenoble, France
[2]CNRM, Université de Toulouse, Météo-France, CNRS, Toulouse, France, 42 avenue Coriolis 31057 Toulouse, France
[3]Univ. Grenoble Alpes, CNRS, IRD, Grenoble INP, IGE, Grenoble, France

Correspondence: Guillaume Evin (guillaume.evin@inrae.fr)

Abstract. Large Multiscenarios Multimodel Ensembles (MMEs) of regional climate model (RCM) experiments driven by Global Climate Models (GCM) are made available worldwide, and aim at providing robust estimates of climate changes and associated uncertainties. Due to many missing combinations of emission scenarios and climate models leading to sparse Scenario-GCM-RCM matrices, these large ensembles are however very unbalanced, which makes uncertainty analyses im-

5 possible with standard approaches. In this paper, the uncertainty assessment is carried out by applying an advanced statistical approach, called QUALYPSO, to a very large ensemble of 87 EURO-CORDEX climate projections, the largest ensemble ever produced for regional projections in Europe. This analysis provides i) the most up-to-date and balanced estimates of mean changes for near-surface temperature and precipitation in Europe, ii) the total uncertainty of projections and its partition as a function of time, and iii) the list of the most important contributors to the model uncertainty. For changes of total precipitation

10 and mean temperature in winter (DJF) and summer (JJA), the uncertainty due to RCMs can be as large as the uncertainty due to GCMs at the end of the century (2071-2099). Both uncertainty sources are mainly due to a small number of individual models clearly identified. Due to the highly unbalanced character of the MME, mean estimated changes can drastically differ from standard average estimates based on the raw ensemble of opportunity. For the RCP4.5 emission scenario in Central-Eastern Europe for instance, the difference between balanced and direct estimates are up to 0.8°C for summer temperature changes and

15 up to 20% for summer precipitation changes at the end of the century.

1 Introduction

Climate change studies usually rely on Multiscenarios Multimodel Multimember Ensembles (MMEs) of transient climate projections. Large MMEs are now available and exploited to assess mean changes and related uncertainties. Among these MMEs, many dynamical downscaled ensembles rely on regional climate models (RCMs) which are used to downscale global

20 climate model (GCM) projection simulations for a given set of scenarios. The added value of regional projections has been demonstrated in many studies (Herrmann et al., 2011; Giorgi and Gutowski, 2015; Rummukainen, 2016; Fantini et al., 2018), particularly in mountainous and complex coastline areas, and for local wind systems and extreme precipitation events.

The European part of the COordinated Regional Downscaling EXperiment (EURO-CORDEX) has led to a very large MME at a 0.11° horizontal resolution, which is so far the largest ensemble ever produced with regional climate models (Jacob et al., 2014; Kotlarski et al., 2014; Coppola et al., 2020; Vautard et al., 2020). As a result of this long-standing effort of the regional climate modelling community, strengthened estimates of future meteorological changes at regional scales can be assessed over Europe and possible impacts of future climate change can be explored at high-resolution. The EURO-CORDEX ensemble also allow to disentangle the different uncertainty sources in projections, namely uncertainties due to the emission scenario, model diversity and natural climate variability (Déqué et al., 2007; Hawkins and Sutton, 2009; Déqué et al., 2012). For regional projections, model uncertainty combines GCM uncertainty (for a same radiative forcing, different GCMs produce different forced responses) and RCM uncertainty (different RCMs forced by a same GCM produce different regional responses). As such, the EURO-CORDEX ensemble provides a good opportunity to estimate the relative contributions of GCMs and RCMs to model uncertainty, and thus to identify the largest uncertainty sources and where modelling forces could be preferentially allocated in the coming years.

The statistical treatment of large MMEs is challenging for different reasons and MMEs composed of EURO-CORDEX climate projections are no exception. Some GCMs are over-represented, a few GCMs being selected by almost all regional climate modelling groups while other GCMs are used for a few experiments only. A similar configuration is found for RCMs. If a few RCMs have been used to downscale a large number of GCMs, most RCMs were applied to small (and often different) GCM subsets. The same applies for emission scenarios. There are about two times more GCM/RCM chains produced for RCP8.5 than for RCP4.5 and RCP2.6.

The unbalanced nature of the EURO-CORDEX ensemble and of all MMEs in general is obviously a side effect of the very large computational efforts needed to produce high-resolution simulations. As a consequence, RCP x GCM x RCM matrices of MMEs are always very incomplete, with missing experiments for many different RCP/GCM/RCM combinations. In the EURO-CORDEX MME considered in this study for instance, 13 RCMs have been used to downscale projections of 9 CMIP5 GCMs for 3 RCP scenarios. From the 3 x 9 x 13 = 357 possible RCP/GCM/RCM combinations, only 87 were available in August 2020. This number is continuously increasing but the matrix of possible RCP/GCM/RCM combinations will never fill up entirely.

Due to the incomplete nature of MMEs, uncertainty analyses cannot be performed with standard ANalysis Of VAriance (ANOVA) approaches. However, this incompleteness issue is usually ignored and mean climate changes are typically estimated by the average of available projections (Jacob et al., 2014; Kjellström et al., 2018; Coppola et al., 2020; Vautard et al., 2020) while Evin et al. (2019) demonstrate that it can lead to incorrect estimates of the mean changes and of the different uncertainty sources. As an alternative solution, other studies sub-sample the MME to obtain a balanced subset of available chains (Tramblay and Somot, 2018; Christensen and Kjellström, 2020). In the analysis of Christensen and Kjellström (2020) for instance, a nearly full submatrix of 19 EURO-CORDEX experiments, made of 5 x 4 GCM/RCM combinations available for RCP8.5, has been considered. The other model combinations and scenarios were thus disregarded. Sub-sampling MMEs leads obviously to a dramatic waste of information (only 20% of available chains were considered in the previous example), and under-representative estimates.

A correct uncertainty assessment of unbalanced MMEs is not straightforward but a few works have been proposed in the last years to tackle this challenging "incompleteness" issue. Northrop and Chandler (2014) propose a random-effects ANOVA model which consider the MME as a sample of a wider population. Other approaches make use of data reconstruction or augmentation techniques (Déqué et al., 2007, 2012; Evin et al., 2019). In the present paper, QUALYPSO, an advanced statistical approach presented in Evin et al. (2019), is applied to EURO-CORDEX projections in order to estimate the mean changes of winter/summer temperature and precipitation over Europe. QUALYPSO applies the "time-series" approach (Hawkins and Sutton, 2009; Hingray and Saïd, 2014) which consists in separating the forced climate response from the internal variability using a trend model. Hingray et al. (2019) show that the precision of all uncertainty estimates is higher with this approach than with the "single time" approach (Yip et al., 2011), i.e. when multiple members are used and exploited to assess the different uncertainties for each future time window. We also estimate the related total uncertainty, the different sources of uncertainties and the individual contribution of each climate model (GCMs and RCMs) to their corresponding uncertainties. In contrast to many previous studies, a large MME of 87 EURO-CORDEX experiments is analysed and all uncertainty sources associated to the ensemble are considered: scenario uncertainty, GCM uncertainty, RCM uncertainty, climate internal variability, as well as the uncertainty related to the different interactions (RCM/GCM, RCM/scenario, GCM/scenario).

The objectives of this paper are thus threefold:

- Provide robust estimates of climate precipitation and temperature changes at high-resolution in Europe for the next decades, thanks to the largest MME of regional climate projections ever produced,

- Provide a robust estimate of total uncertainty and of its different components,

- Identify the individual climate models which contribute the most to model uncertainty.

Note that the term "robust" here indicates that obtained estimates are not sensitive to the available RCP/GCM/RCM combinations for the same sets of scenarios and climate models. It must not be confused with the notion of statistical robustness which aims at providing estimates less sensitive to outliers or departures from standard assumptions (e.g. normality).

Section 2 presents the MME composed of EURO-CORDEX climate projections used in this study. Section 3 describes the methodology proposed for estimating mean projected changes and partitioning climate change uncertainties. Sections 4 and 5 then show mean changes and related uncertainties for illustrative regions and for entire Europe, respectively. In sections 6 and 7, we then focus on the contributions of the main sources of uncertainty, and of the individual climate models. Section 8 then discusses these results. Section 9 concludes.

2   EURO-CORDEX climate projections

This study exploits the outputs of the EURO-CORDEX initiative (Jacob et al., 2014, 2020) which is composed of climate experiments obtained from thirteen (13) RCMs forced over Europe by nine (9) CMIP5 GCMs (Taylor et al., 2011) for the historical, RCP2.6, RCP4.5 and RCP8.5 emission scenarios (Moss et al., 2010). Most historical runs cover the period 1950-2005 and runs obtained with the different RCPs cover the period 2006-2099. Table 1 lists the 87 RCP/GCM/RCM modelling

RCM \ GCM	CanESM2	CNRM CM5	EC EARTH	HadGEM2 ES	IPSL - CM5A-MR	MIROC5	MPI - ESM-LR	NorESM1 M	GFDL ESM2G
REMO	○	○	⊗	⊗		⊗	⊛	⊗	×
CCLM4-8-17	○	⊕	⊛	⊕		⊗	⊛		
ALADIN63		⊛		○					
RACMO22E		⊛	⊛	⊛	○		○	○	
HIRHAM5		○	○	⊕			○	⊕	
WRF381P		○		○	⊕			○	
RCA4		⊕	⊛	⊛	⊕		⊛	⊗	
WRF361H			○	○		○	⊗		
RegCM4-6				⊗			○		
COSMO-CLIM							○	○	
ALARO-0		⊛							
ALADIN53		⊛							
HadREM3-GA7				○					

Table 1. Combination of available GCM and RCM pairs with the scenarios RCP2.6 (×), RCP4.5 (+) and RCP8.5 (○).

90 chains available in August 2020 and used in the present study (see also the full characteristics of the scenarios in Table S1 of the SM). 21 chains have been obtained with the RCP2.6, 19 with the RCP4.5, and 47 with the RCP8.5. For each chain, time series of mean temperature and total precipitation, aggregated at seasonal (DJF and JJA) scales and averaged over 30-year moving windows, and at a $0.11°$ resolution (which corresponds to $424 \times 412 = 174\,688$ grid points) have been extracted.

Note that we consider REMO2009 and REMO2015 as only one RCM but both versions of ALADIN and CCLM as different
95 RCMs as advised (Vautard et al., 2020). An error has been detected in the atmosphere lateral boundary condition files provided initially for the simulation historical_r1i1p1 of the CNRM-CM5 CMIP5 model. The atmosphere data at the 6-hourly frequency on the model level (6hLev) used for driving the regional climate models do not come from the member r1i1p1 whereas the SST does. The RCMs ALADIN53, CCLM4-8-17, RCA, REMO, ALARO-0 use the erroneous CNRM-CM5 lateral boundary conditions whereas the RCMs ALADIN63, RACMO22E, HIRHAM5, WRF381P use the corrected version. This error has
100 likely no significant effect on the multi-annual climate change signal. As a consequence, following Vautard et al. (2020), this study considers all the runs obtained with the CNRM-CM5 CMIP5 model. Other known issues in EURO-CORDEX simulations can be found in the errata page (https://www.euro-cordex.net/078730/index.php.en).

3   Statistical assessment of mean changes and uncertainty sources

Mean changes and associated uncertainty components are estimated with the QUALYPSO approach described in Evin et al.
105 (2019). The QUALYPSO approach applies data augmentation techniques in order to assess uncertainties in incomplete MMEs.
Scenario and model uncertainty is obtained with a fixed effects ANalysis Of VAriance (ANOVA) applied to the ensemble of
climate change responses estimated for the different chains. The time evolution of the forced response of any given chain
is assumed to be gradual and smooth, the higher-frequency variations of the time series being due to internal variability of
the studied variable alone (the so-called quasi-ergodicity assumption, see Hingray and Saïd, 2014). The forced response of a
110 particular simulation chain for a given emission scenario is thus considered to correspond to the long-term trend of the climate
projections.

For a detailed description of the QUALYPSO method, we refer to Evin et al. (2019). Details on the method applied in this
study are provided in Section 2 of the supplementary materials. The different steps can be summarized as follows :

- **Forced response:** The forced response is estimated for each of the 87 climate simulations by fitting a trend model using
115 a cubic smoothing spline (implemented by the function `smooth.spline` in R software, R, 2017). High smoothing
parameters (`spar` argument of `smooth.spline` equals to 1.1 for temperature and 1 for precipitation, respectively)
are chosen in order to avoid including decennial variability into these fitted forced responses.

- **Climate change response:** The climate change response corresponds to the anomaly of the forced response between a
future period and the 1981-2010 reference period. Absolute changes are considered for temperature, relative changes for
120 precipitation.

- **Main ANOVA effects:** Using an ANOVA method combined to data augmentation techniques implemented within a
Bayesian framework, estimates of the mean change of the MME and the main effect of each GCM, each RCM and
each RCP scenario are obtained. The main effect of a GCM corresponds to the mean deviation of all RCP/GCM/RCM
chains obtained with this GCM from the mean change of the MME, with a proper treatment of missing RCP/GCM/RCM
125 combinations.

- **Interaction effects:** The deviations between the climate change responses and the sum of the mean ensemble change
and the main effects are further decomposed in order to estimate three types of interactions between models/scenarios:
RCM/GCM, RCM/RCP and GCM/RCP.

- **ANOVA decomposition:** The dispersion (variance) between the main effects obtained for the different GCMs, the
130 different RCMs and the three RCP scenarios give an estimate of the GCM uncertainty, the RCM uncertainty and the
scenario uncertainty, respectively. Similarly, the variance between the interaction effects provide the uncertainty related
to RCM/GCM, RCM/RCP and GCM/RCP interactions.

- **Residual variability:** The residual variability corresponds to the part of the total variance which cannot be attributed to
the other sources of uncertainty (i.e. related to the main effects, to the different interactions, or to internal variability).

135   – **Internal variability:** The internal variability component of the MME is estimated as the multimodel mean internal variability, where the internal variability of each chain is estimated as the temporal variance of the deviations of raw climate projections from the climate change responses of the chain.

QUALYPSO provide estimates of different quantities, among which:

    – **BM$_\mathbf{k}$ ("Balanced" mean change response):** The "balanced" mean climate change response for each RCP scenario k
140   ('long-term' anthropogenic signal), i.e. the sum of the balanced mean change response of the whole MME, $\hat{\mu}(t)$ and of the main effect of that scenario k, $\hat{\gamma}_k(t)$ (see Eq. S3 in the SM).

    – **Total Variance:** The total variance in projections for the whole ensemble is the sum of the variances corresponding to scenario uncertainty, GCM and RCM uncertainties, RCM/GCM, RCM/RCP and GCM/RCP interaction uncertainties, residual variability and internal variability, see Eq. S4 in the SM.

145   – **BU ("Balanced" uncertainty):** Scenario-excluded uncertainty (i.e. the standard deviation of the total variance without the uncertainty associated to the scenario, see Eq. S9 in the SM).

    – The relative contribution of the different uncertainty sources to the total variance, as well as the contribution of each individual GCM (resp. RCM) to the GCM (resp. RCM) uncertainty.

For each scenario, the "balanced" mean change response obtained from QUALYPSO, BM_k, results from a proper treatment
150 of missing RCP/GCM/RCM combinations, and can be opposed to the direct estimate of the mean change response M_k taken as the direct average of the raw climate change responses (anomalies between future and reference periods).

The QUALYPSO approach is accessible through the R-package `QUALYPSO` available at the CRAN repository https://CRAN. R-project.org/package=QUALYPSO. The package includes functions that implement the different steps described above, process the outputs and provide a suite of plotting tools. A detailed description of the package and of its features is available in its
155 accompanying documentation.

In the following, we quantify mean changes and uncertainty sources for each grid cell of the EURO-CORDEX domain. Applications are done on 30-year moving averages of mean temperature and total precipitation aggregated for the summer (JJA) and winter (DJF) seasons. In this study, internal variability can thus be interpreted as the low-frequency variability of the climate. It does not include the high-frequency inter-annual variability. In addition, we assess the "significance" of
160 changes for each RCP scenario k by comparing the mean climate change response BM_k to the uncertainty BU. The term "significance" should not be interpreted here as a result of a proper statistical test (see discussion in Section 8). However, an absolute BM_k/BU ratio greater than 1 indicates a certain level of consistency between the climate models, so that the signal provided by the estimated mean climate change response BM_k is considered clear enough to be interpreted (see, e.g. Christensen et al., 2019; Matte et al., 2019). In addition, 90% Gaussian confidence intervals are used as a descriptive tool (i.e.
165 intervals $[BM_k - 1.645\,BU, BM_k - 1.645\,BU]$ are shown). Finally, it must be noted that the scenario-excluded uncertainty BU includes the natural and irreducible climate variability (internal variability), and does not only represent the agreement between the climate models.

4 Mean changes and related uncertainties for illustrative regions

We first assess mean changes and related uncertainties of mean temperature and total precipitation in winter and summer,
170   averaged over three large regions (land and sea points) considered in the IPCC SREX report (Seneviratne et al., 2012), namely
North Europe (NEU), Central Europe (CEU) and South Europe and Mediterranean (MED) (Fig. 1).
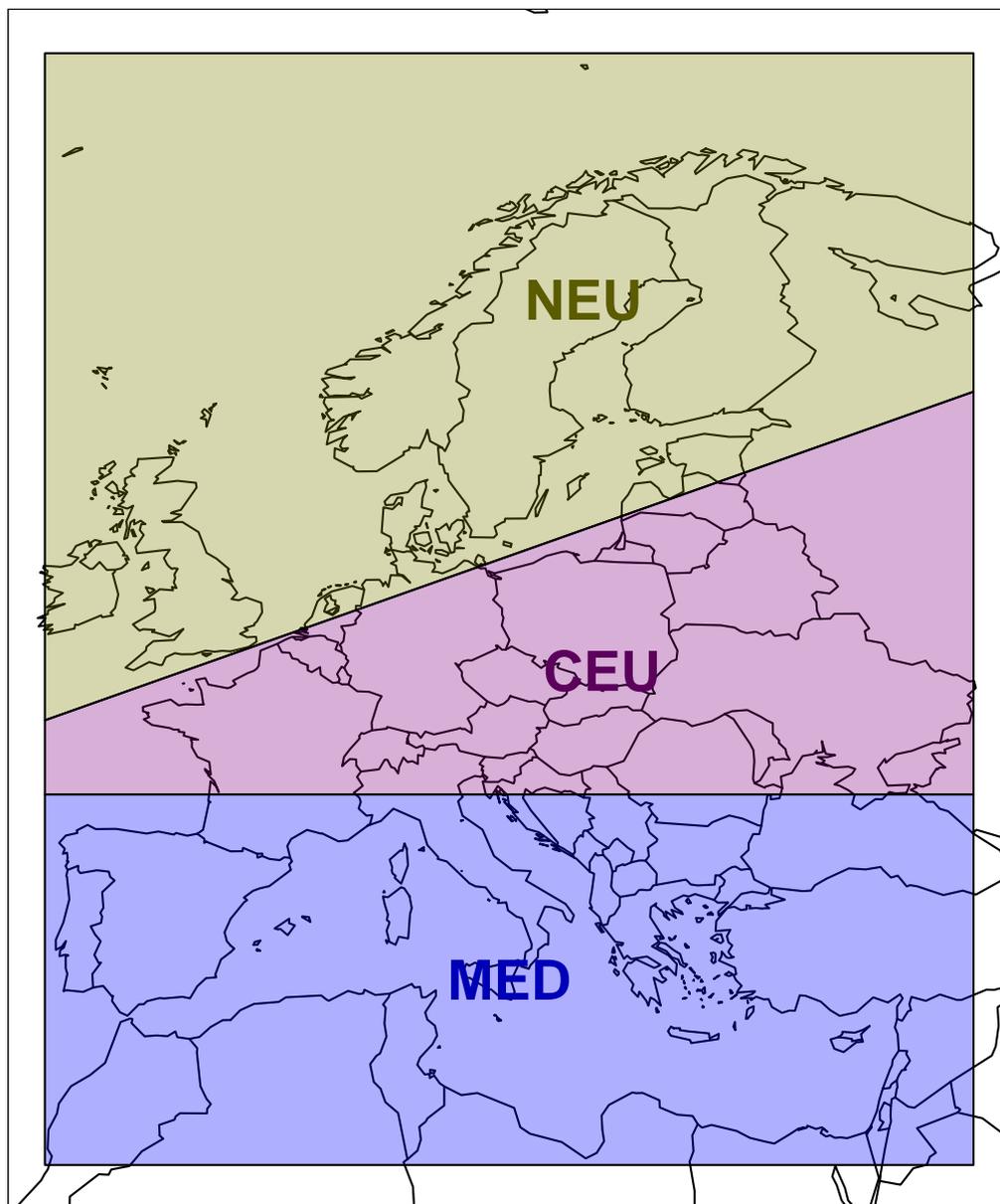
Figure 1. Regions considered in the analyses. The three colored regions are taken from the IPCC SREX report (Seneviratne et al., 2012).

For temperature and precipitation changes in winter and summer, the individual change responses obtained for the different chains, the mean change response BM_k obtained for each scenario k, the scenario-excluded uncertainty BU and, finally, the contribution of the different uncertainty components to the total variance are presented as a function of time for the 3 regions in Figures 2- 5. For both temperature and precipitation, looking at the ensembles of climate change responses (column 1), the largest changes are obtained with the scenario RCP8.5. With this scenario, a steady warming is projected throughout the 21st century, up to around 4°C for the last 30-year period (2071-2099). In addition, Tables 2-5 provide the corresponding numbers and can be used to obtain intervals indicating the related uncertainties. For example, concerning temperature changes in winter and for the period 2071-2099, the 90% uncertainty bands provided in Fig. 2 are thus [2.0, 5.6]°C, [2.5, 5.1]°C and [2.3, 4.0]°C in NEU, CEU and MED regions, respectively, with the RCP8.5. In contrast, with the RCP2.6, warmings are moderate ([-0.6, 3.0]°C, [-0.1, 2.4]°C and [0.3, 2.0]°C for NEU, CEU and MED regions, respectively). The ensemble of climate change responses are very dispersed, and some chains stand out from the others. One chain even simulates a temperature decrease for NEU (see top-left panel in Fig. 2). In winter and with the scenario RCP85, NEU and CEU are warming substantially more than the MED area likely due to the Arctic warming amplification and to the regional snow-albedo positive feedback. Winter precipitation increases by [1%, 21%] in NEU, [5%, 25%] in CEU and decreases by [-19%, 1%] in the MED region with the RCP8.5, see Figure 3. In summer, with the RCP8.5, the projected warming is slightly more intense than in winter for CEU and MED regions (by about 0.3°C), and more moderate in NEU. For summer precipitation, an important decrease can be noticed in the MED region ([-0.55%, 0.0%]), with a rather large uncertainty.

The mean change response BM_k obtained for each scenario k can be put in perspective with the associated uncertainty BU and its different components (columns 2-4). For winter temperature (Fig. 2), the projected warming is clearly marked for the RCP4.5 and RCP8.5 in the three regions, despite an important associate uncertainty. From mid-century, GCM uncertainty clearly overcomes all other sources of uncertainty in the three regions. For winter precipitation (Fig. 3), mean changes are rather moderate in comparison of the different uncertainties, in particular GCM and RCM uncertainties. In Northern and Central Europe, GCM uncertainty is about twice bigger than RCM uncertainty. RCM contribution is small in Southern Europe. For both variables, internal variability dominates during the first decades and rapidly decreases. Except for summer precipitation, the contribution of the different interactions and of the residual variability is moderate, especially for temperature changes. For these cases, the climate change response of each chain is thus adequately represented by a simple additive combination of the main effects (scenario, GCM and RCM). For summer precipitation, interactions between GCM and RCM are not negligible, especially in CEU, and RCP/GCM uncertainty is greater than the residual variability in the three regions. For each scenario k, the balanced mean changes of the ensemble BM_k (white curves) can be compared to the direct averages M_k (thick colored curves), see corresponding differences in Tables S18-S19 of the SM for temperature and precipitation changes, respectively. These differences are more important in summer (e.g. 0.5°C for mean temperature changes in CEU with the scenarios RCP2.6 and RCP4.5, see Table S18 of the SM).

The last columns show the decomposition of the total variance (including the scenario uncertainty). For winter temperature, while scenario uncertainty is dominant in the MED and CEU regions at the end of the century (73% and 66% respectively, see Tab. 2), it is close to the GCM uncertainty in NEU (45% and 48% for GCM and RCP uncertainty, resp.). For winter

precipitation, GCM and scenario uncertainties are similar in the MED and NEU regions at the end of the century, and exceed RCM uncertainty, especially in the MED region. In NEU and CEU, RCM uncertainty is not negligible and can reach the two-thirds of GCM uncertainty. In summer (see Figs. 4 and 5), conclusions are globally similar. However, for summer precipitation, RCM uncertainty exceeds GCM uncertainty in NEU at the end of the century, and contributes to 30% of the total variance in CEU.

Table 2. Balanced mean change response BM_k for each RCP scenario, scenario-excluded uncertainty BU and partition of the total variance for 3 illustrative regions, for absolute changes of mean temperature in winter (DJF) for two future periods compared to the period 1981-2010. I1, I2 and I3 refer to RCM/GCM, RCM/RCP and GCM/RCP interactions, respectively. IV and RV refer to internal and residual variability, respectively. Absolute mean changes greater than the uncertainty ($|BM_k/BU| > 1$) are indicated in bold font. 90% confidence intervals can be obtained with the expression $[BM_k - 1.645\,BU, BM_k - 1.645\,BU]$.

BM_k and BU (°C)				% Total variance							
RCP			BU	Main effects			Inter.				
2.6	4.5	8.5		RCM	GCM	RCP	I1	I2	I3	IV	RV
2021-2050											
NEU **1.0**	**1.2**	**1.6**	0.5	8	66	17	3	0	2	4	1
CEU **0.9**	**1.1**	**1.4**	0.3	9	36	27	5	1	5	15	3
MED **0.8**	**0.9**	**1.2**	0.2	5	51	32	1	0	4	6	1
2071-2099											
NEU **1.2**	**2.4**	**3.8**	1.1	3	45	48	1	0	2	1	0
CEU **1.1**	**2.2**	**3.8**	0.8	5	21	66	1	1	4	1	1
MED **1.1**	**1.8**	**3.1**	0.5	2	23	73	0	0	1	1	0

Table 3. Same as Tab. 2 for relative changes of total precipitation in winter (DJF).

BM_k and BU (%)				% Total variance							
RCP			BU	Main effects			Inter.				
2.6	4.5	8.5		RCM	GCM	RCP	I1	I2	I3	IV	RV
2021-2050											
NEU 1	3	**4**	3	24	43	11	3	1	3	14	2
CEU 3	**4**	**6**	3	15	33	13	1	1	3	34	1
MED 0	-2	**-3**	3	8	27	22	3	0	4	33	3
2071-2099											
NEU 2	6	**11**	6	23	40	26	2	1	3	3	1
CEU **6**	**8**	**15**	6	21	29	31	2	1	4	9	3
MED 2	-5	**-9**	6	7	36	37	4	1	7	6	3
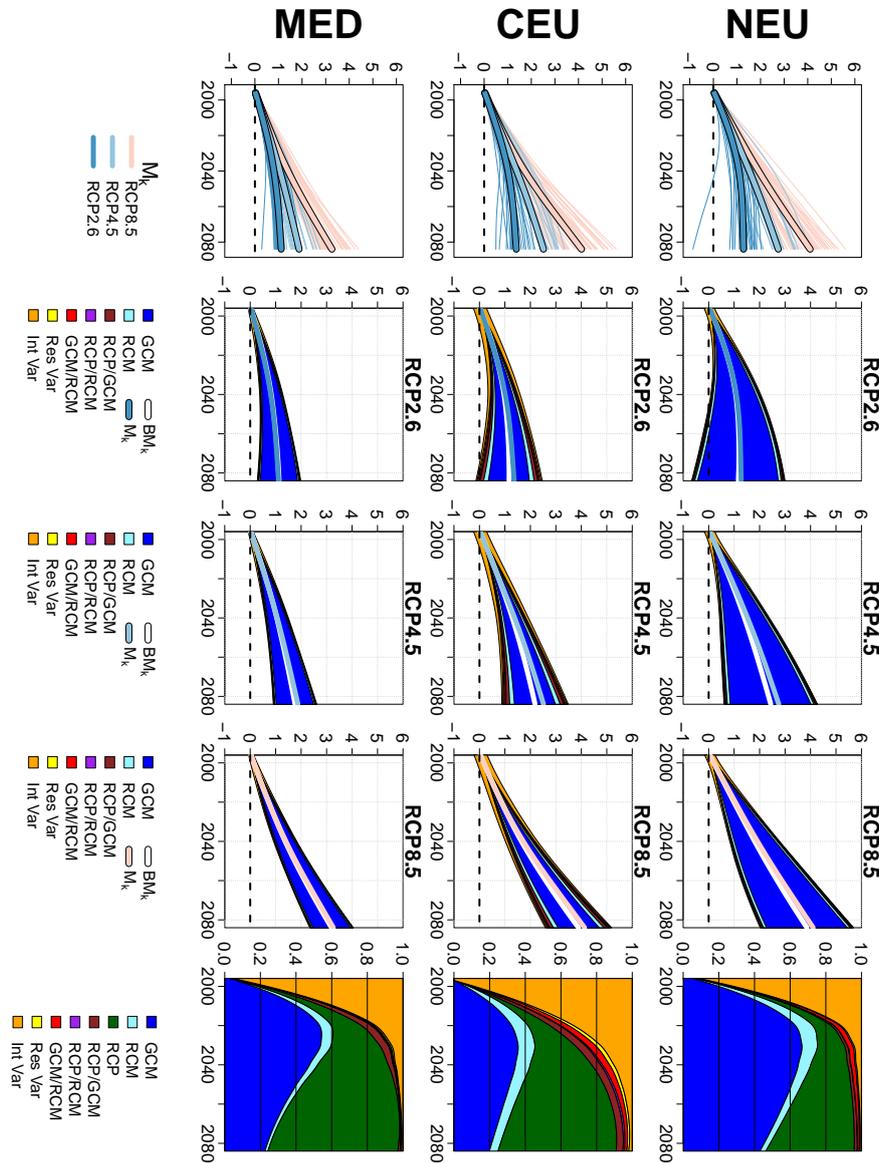
Figure 2. Balanced mean climate change responses BM_k of absolute changes of mean temperature in winter (DJF) as a function of time and related uncertainties compared to the period 1981-2010, for 3 illustrative regions (see Fig. 1). Column 1: Ensembles of climate change responses for each RCP scenario, thick lines represent the direct mean response M_k, i.e. the direct average of each ensemble. Columns 2-4: For each scenario, the balanced mean change BM_k obtained with the QUALYPSO approach (thick white line), can be compared with the direct average M_k (thick colored line), as shown in the first column, and corresponding 90% uncertainty band. The width of the overall colored interval represents the different sources of uncertainty corresponds to $BM_k \pm 1.645 BU$. This interval is subdivided into subintervals whose width is proportional to the fraction of total variance explained by the different sources of uncertainties. Column 5: fraction of total variance.
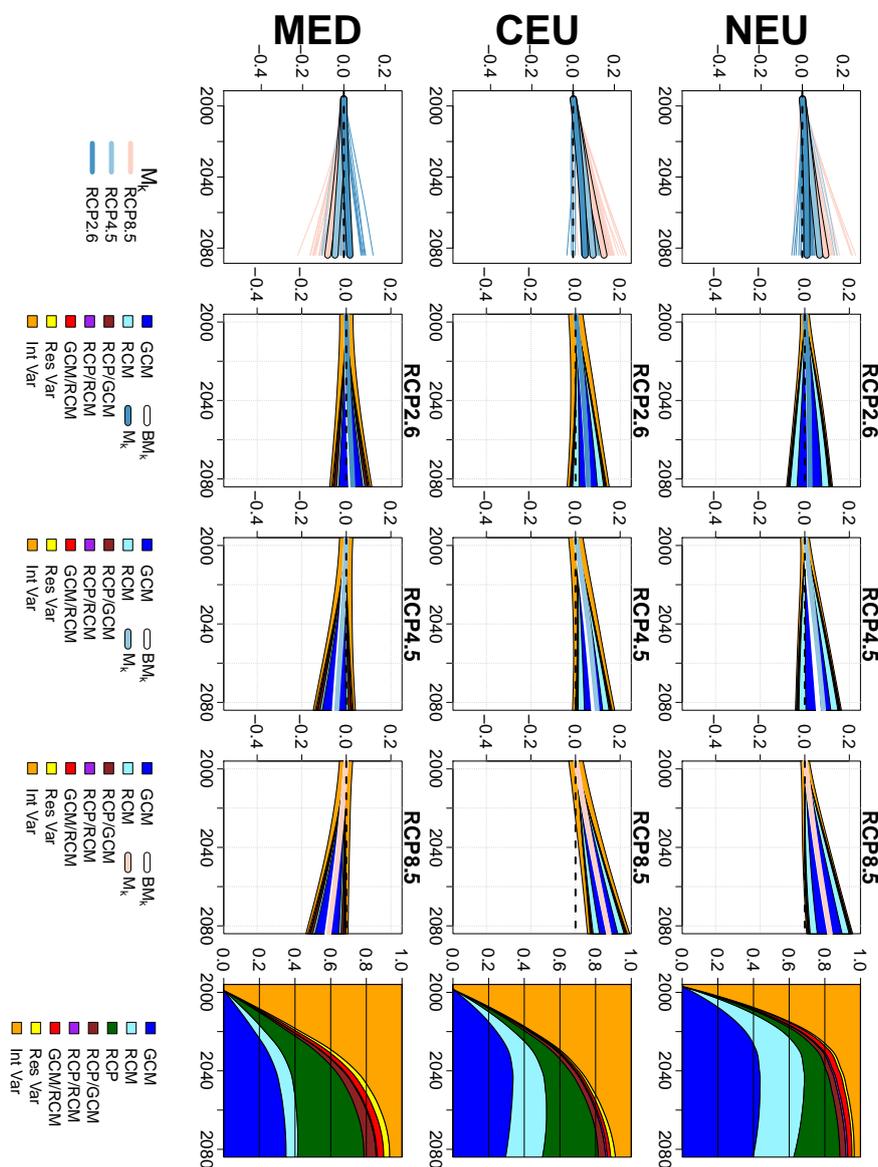
Figure 3. Same as Fig. 2 for relative changes of total precipitation in winter (DJF).

Tables S2-S9 of the SM provide the same quantitative results for all the countries of domain, for absolute temperature and relative precipitation changes, in winter and summer, for the near future (2021-2050) and at the end of the century (2071-2099). Tables S10-S17 of the SM report the same summary for all capital cities of the domain.

215 At the scale of the countries, the projected warming for the period 2071-2099 in winter (Table S3 of the SM) varies between between 0.4°C and 1.9°C for RCP2.6, between 1.2°C and 3.6°C for RCP4.5 and between 2.2°C and 5.7°C for RCP8.5. The largest changes are obtained for Scandinavian countries (Finland, Norway). For most countries, the mean precipitation change in winter at the end of the century (Table S5 of the SM) for RCP2.6 is moderate compared to the uncertainty, the
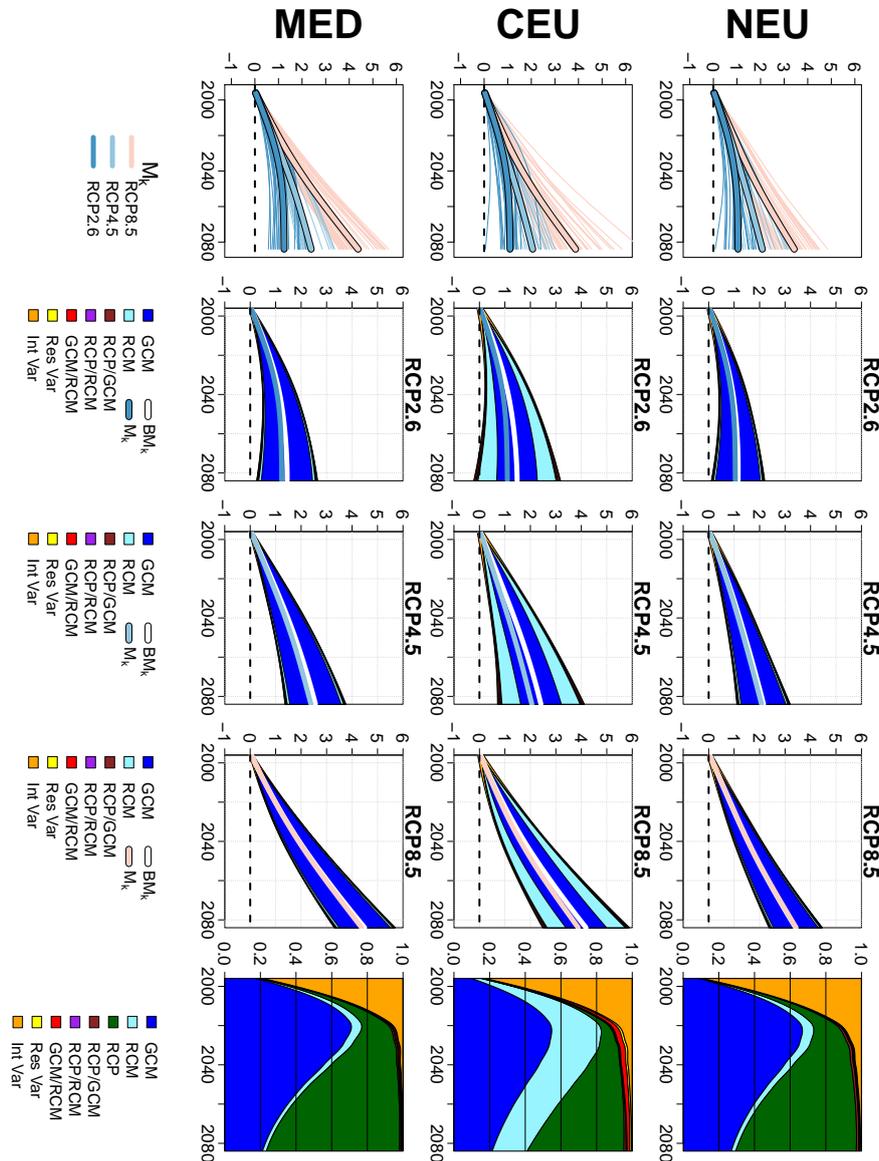
Figure 4. Same as Fig. 2 for absolute changes of mean temperature in summer (JJA).

absolute response-to-uncertainty ratio $|BM_k/BU|$ being less than one. The estimated mean changes are stronger for RCP4.5.

220 For RCP8.5, a clear increase is estimated for countries in Northern and Central Europe, and a clear decrease in the South of Europe (e.g. Cyprus, Morocco, Tunisia). The next section will detail the spatial variability of these changes and in section 6, we comment the spatial variability of the main contributions to the total variance.

Here, we can notice that the spatial scale (i.e. country versus capital) has an effect on the magnitude of the uncertainty and its different components. For example, looking at the precipitation changes in winter in 2071-2099 for the countries (Table S5 in the SM) and the capitals (Table S13 in the SM), the uncertainty BU increases from 6% and 10% for France and Greece,
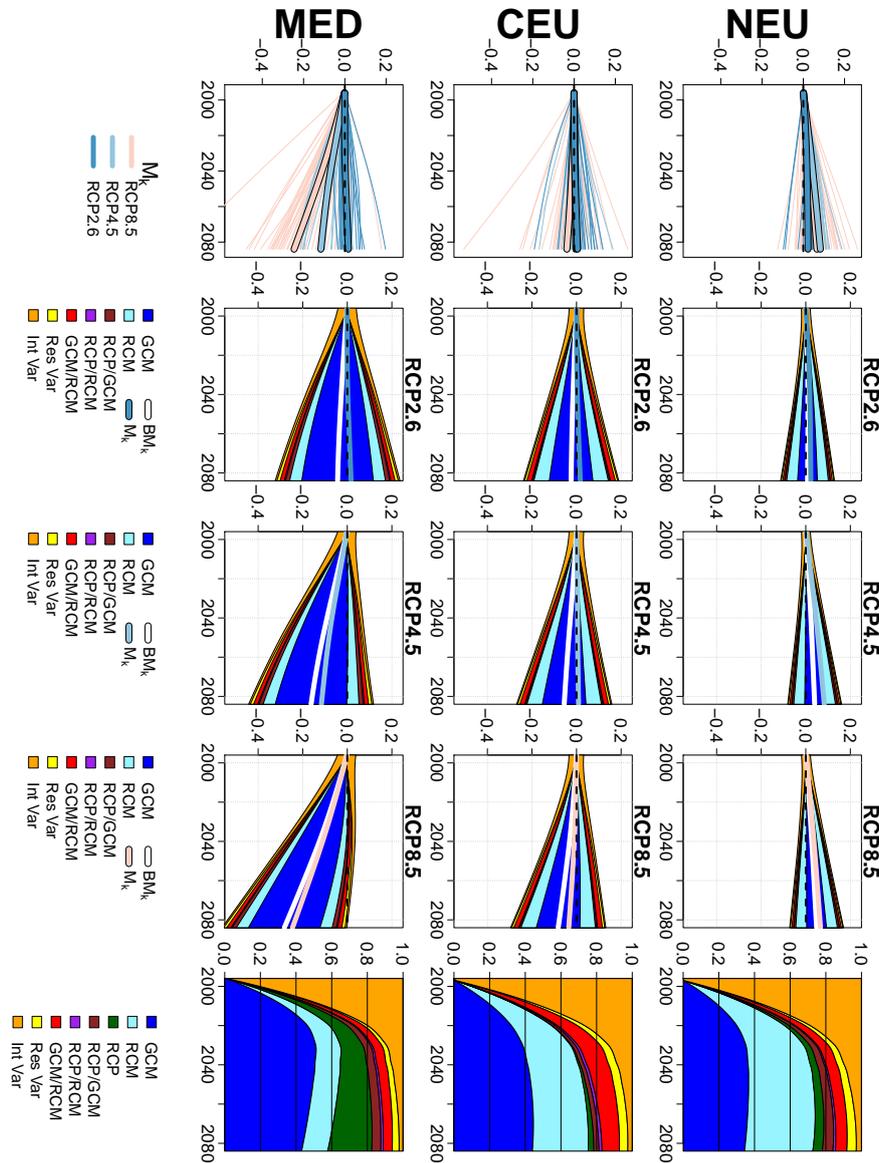
Figure 5. Same as Fig. 2 for relative changes of total precipitation in summer (JJA).

respectively, to 9% and 16% for their capitals Paris and Athens, respectively. The same kind of increase can be observed for the internal variability of precipitation changes. For example, for precipitation changes in winter, the square root of the internal variability increases from 2.6% and 3.3% for France and Greece to 3.1% and 4.9% for Paris and Athens, respectively. The spatial scale has thus a general impact on the different uncertainties, internal variability being generally known to increase at 230 smaller space scales, as shown in previous studies (see, e.g. Hawkins and Sutton, 2009). In addition, it can be noticed that although this increase is marked for precipitation changes, it is almost absent for temperature changes in this study (results not shown).

Table 4. Same as Tab. 2 for absolute changes of mean temperature in summer (JJA).

BM_k and BU (°C)				% Total variance							
RCP			BU	Main effects			Inter.				
2.6	4.5	8.5		RCM	GCM	RCP	I1	I2	I3	IV	RV
2021-2050											
NEU **0.9**	**1.1**	**1.3**	0.3	6	61	25	1	0	1	5	0
CEU **1.0**	**1.2**	**1.5**	0.5	26	52	13	3	0	1	3	1
MED **1.1**	**1.3**	**1.6**	0.4	5	62	29	1	0	1	2	0
2071-2099											
NEU **1.2**	**2.1**	**3.4**	0.6	3	28	66	0	0	1	0	0
CEU **1.5**	**2.4**	**4.1**	1.0	21	22	53	1	1	1	0	1
MED **1.5**	**2.5**	**4.4**	0.7	2	22	74	0	0	1	0	0

Table 5. Same as Tab. 2 for relative changes of total precipitation in summer (JJA).

BM_k and BU (%)				% Total variance							
RCP			BU	Main effects			Inter.				
2.6	4.5	8.5		RCM	GCM	RCP	I1	I2	I3	IV	RV
2021-2050											
NEU 1	2	2	3	35	35	3	6	1	4	13	4
CEU -1	-2	-3	6	28	40	1	12	1	2	11	5
MED -2	-8	**-11**	9	14	50	14	5	1	4	9	3
2071-2099											
NEU 1	4	5	7	38	34	5	7	2	6	3	5
CEU -3	-6	-8	13	30	46	3	10	2	3	2	5
MED -4	-16	**-28**	17	15	43	24	5	1	5	2	4

5   Spatial variability of mean changes and related uncertainty.

Figures 6 and 7 show the estimated mean climate change response BM_k of temperature and precipitation obtained for the
235   periods 2021-2050 and 2071-2099, respectively, for the three RCP scenarios and for both winter and summer seasons. Only
areas where the response stands out from the uncertainty ($|BM_k/BU| > 1$) are shown.

For the near future (Fig. 6), estimated temperature changes are quite similar between the scenarios, the warming being
slightly more intense with the RCP8.5 (between 0.5°C and 2°C) than with the RCP2.6 and RCP4.5 (between 0°C and 1.5°C).
For the period 2021-2050, regions where projected precipitation changes are more important than the uncertainty are mostly
240   obtained with the RCP8.5, with an increase between 5% and 15% in the North of Europe in winter, a decrease between 5% and
35% in Morocco and Algeria in winter, and a decrease between 5% and 15% in summer over the West of Europe (Portugal,
Ireland).

If we now look at the end of the century (Fig. 7), estimated mean warming varies from 0°C to 2°C for RCP2.6, from 2°C
to 4°C for RCP4.5 and from 4°C to 5.5°C for RCP8.5. With the RCP8.5, the strongest increases (by more than 5°C) are in
245   the North-East of Europe (Scandinavia, Russia) in winter, and in the South in summer (land areas around the Mediterranean
sea). Higher warming rates are noticeable in winter with the RCP8.5 for some mountain ranges (Alps, Pyrenees, Carpathian,
Atlas, part of Turkey). In summer, under the RCP8.5 hypothesis, an attenuated warming can be noticed along the coastlines of
France, Spain and South Mediterranean countries.

For precipitation, at the end of the century, only mild changes in a few regions can be noticed for the scenario RCP2.6
250   (e.g. around the Alps in winter). With the RCP4.5, a slight increase (between 5% and 15%) is projected in the North of
Europe in winter and some decreases are projected for small areas (e.g. around Morocco in winter, in Portugal, North of
Spain, West of France and Turkey in summer). With the RCP2.6 and RCP4.5, estimated changes are thus usually moderate
in comparison of the uncertainty. With the RCP8.5 however and in accordance to Coppola et al. (2020), the bipolar pattern
is stronger in both seasons with an increase of precipitation in the North of Europe (with areas higher than +35% in winter)
255   and a decrease in the South (with areas lower than -35% in both seasons). The demarcation between regions with decreasing
or increasing precipitation trends (in white) shifts northwards in summer and southwards in winter. In France and in the UK,
decreases are thus projected in summer, and increases in winter. We can also notice that the decrease in precipitation in summer
with the RCP8.5 scenario over most of the Mediterranean islands (Majorca, Corsica, Sardinia, Sicily, Crete, Rodos, Cyprus) is
stronger than for the surrounding sea areas. This specific local climate change information relevant for the island water resource
260   issue could not be provided by lower-resolution climate models (i.e. GCMs, or RCMs at coarser resolutions). It is also worth
mentioning the East-West asymmetry for Central Italy in the summer precipitation response with the RCP8.5, at the end of the
century, confirming the pioneer study by Gao et al. (2006).

Figure 8 presents the scenario-excluded uncertainty BU in projections by the end of the century. For temperature, this
uncertainty varies between 0.4°C to 2°C. It is larger in the North-East of Europe in winter where it can reach up to 2°C and
265   over the continental part of Eastern Europe in summer. Over the sea, the uncertainty is strong in the Norwegian Sea, in the
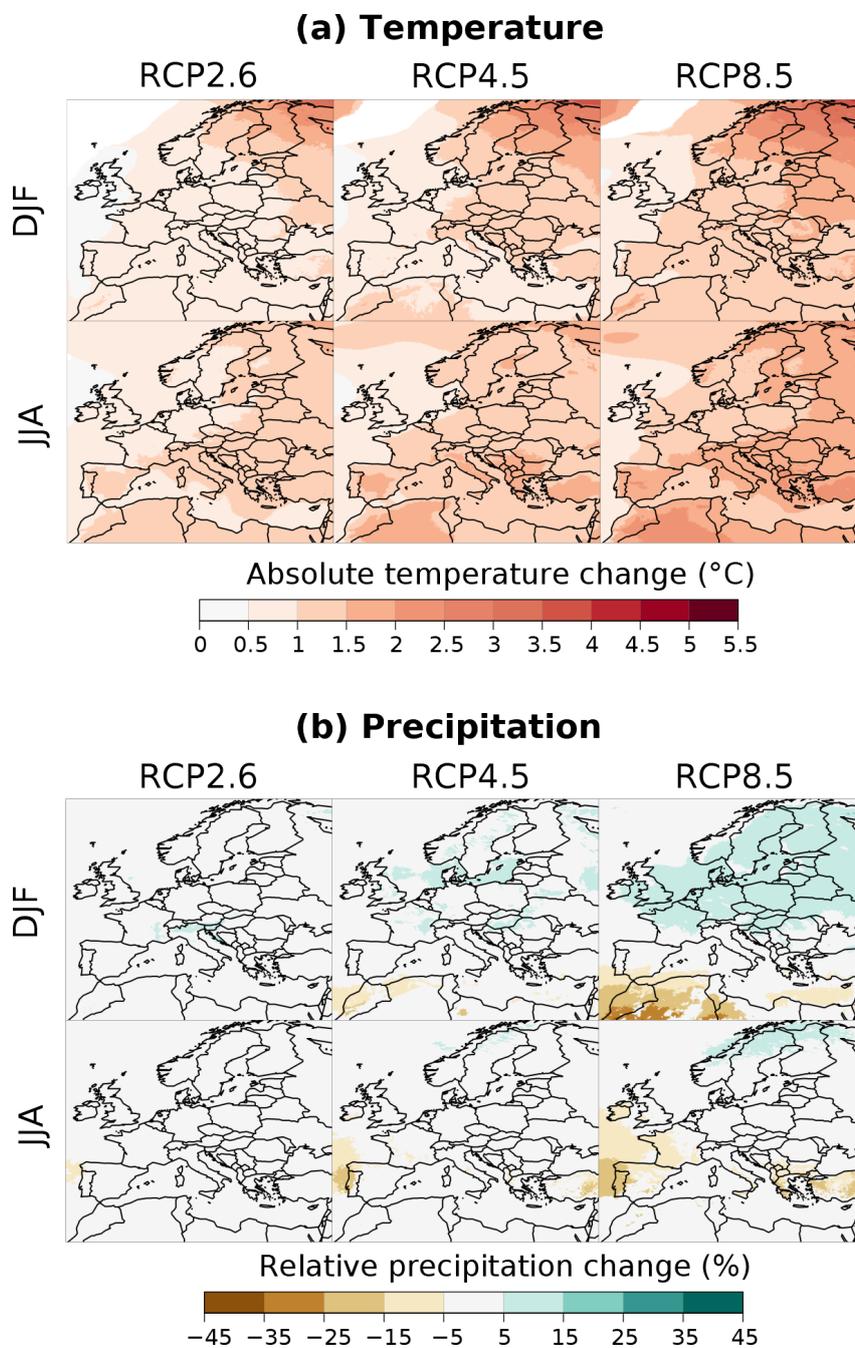
Figure 6. Balanced mean climate change response BM_k obtained with the different RCP scenarios for the near future (2021-2050) compared to the period 1981-2010 in winter (DJF) and summer (JJA). (a) Absolute changes of temperature. (b) Relative changes of precipitation. Only areas where the absolute response-to-uncertainty ratio is greater than 1 ($|BM_k/BU| > 1$) are shown.
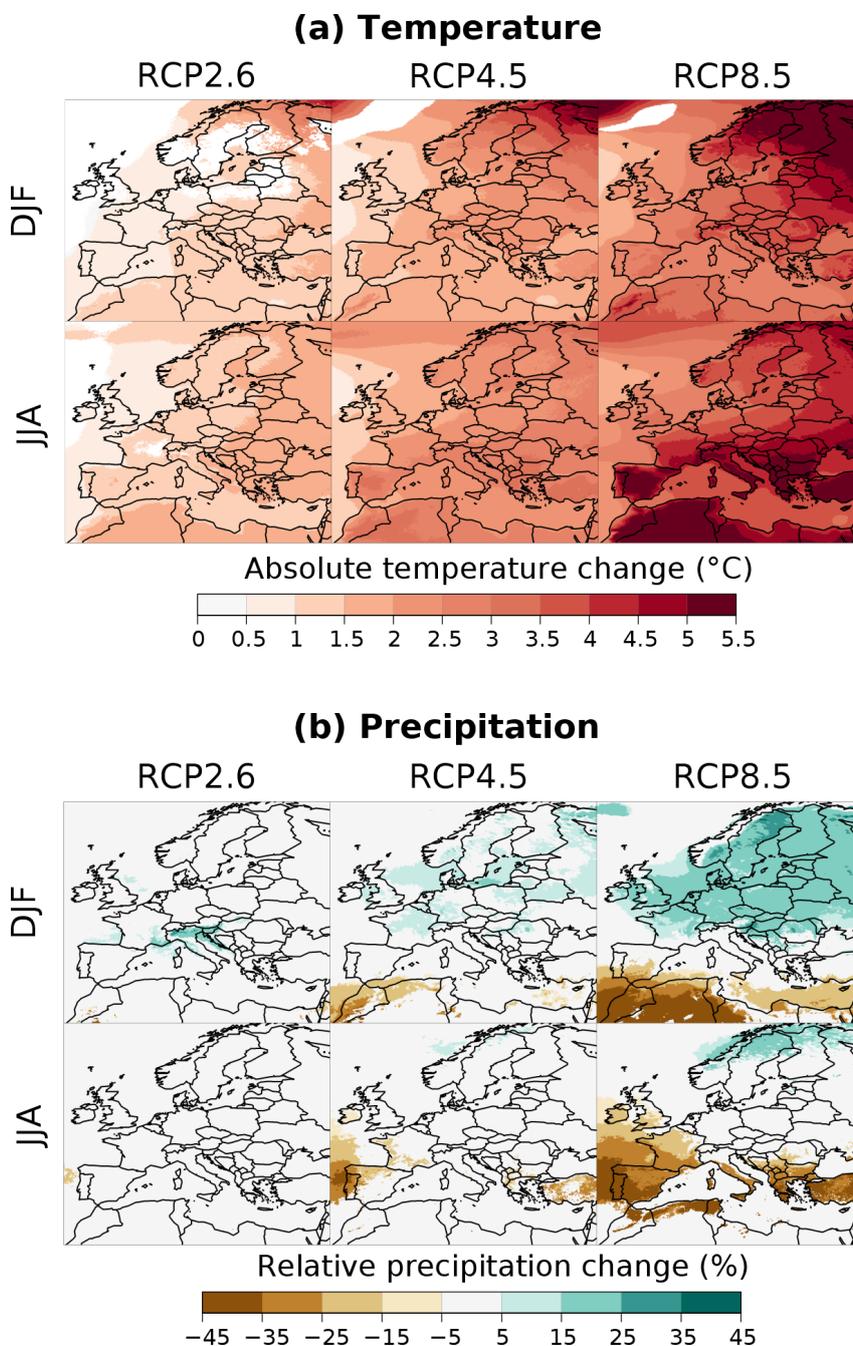
Figure 7. Balanced mean climate change response BM_k obtained with the different RCP scenarios at the end of the twenty-first century (2071-2099) compared to the period 1981-2010 in winter (DJF) and summer (JJA). (a) Absolute changes of temperature. (b) Relative changes of precipitation. Only areas where the absolute response-to-uncertainty ratio is greater than 1 ($|BM_k/BU| > 1$) are shown.

North and East of the Baltic Sea as well as in the Aegean and Adriatic Seas in summer, pointing out the role of the ocean component of the driving GCMs through the change in sea ice cover and sea surface temperature.

For precipitation, the scenario-excluded uncertainty is almost everywhere less than 15-20% in winter and less than 20-25% in summer. The largest values are obtained in North Africa, in the Norwegian Sea and the Arctic Ocean in winter. In summer, the high values are found over the Mediterranean, Black and Baltic seas and in North Africa, the Mediterranean climate zones in Italy, France, Spain, Turkey and Mediterranean islands.
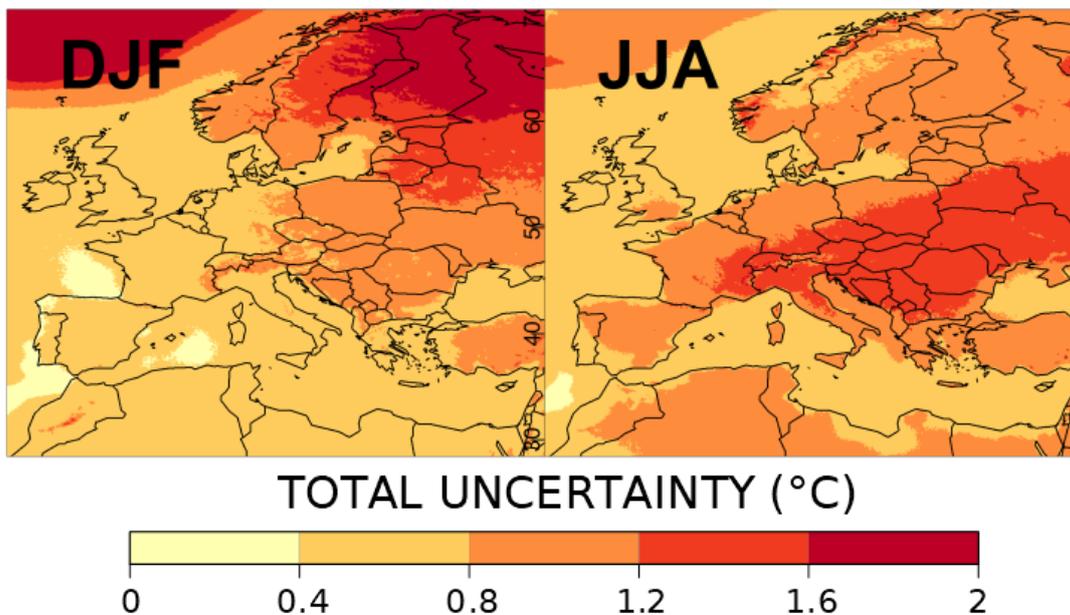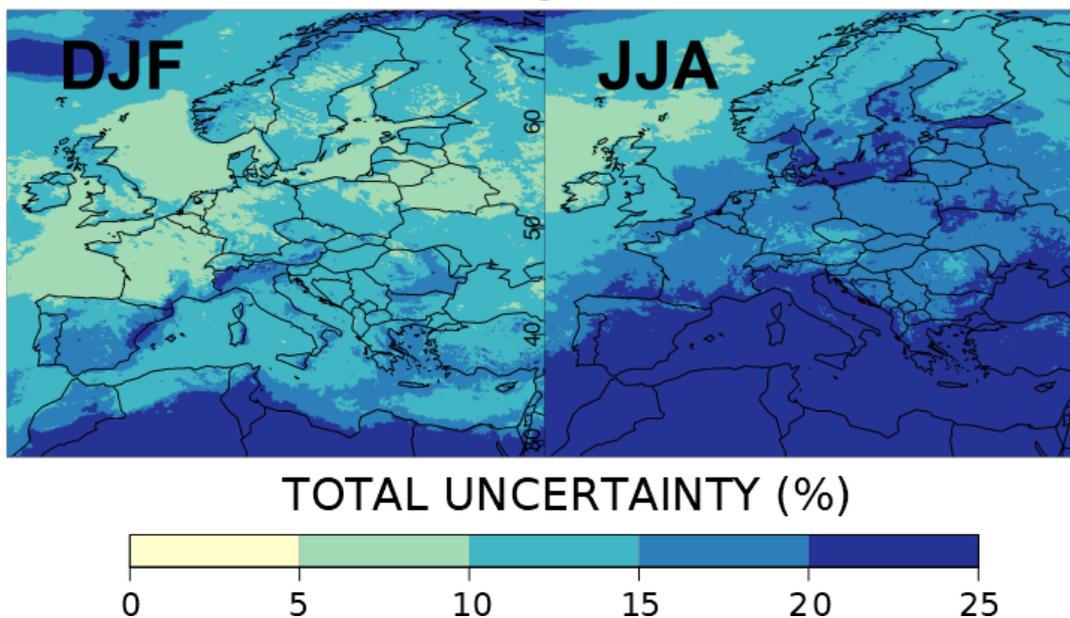
Figure 8. Scenario-excluded uncertainty (balanced estimates) *BU* of the climate change responses at the end of the twenty-first century (2071-2099) compared to the period 1981-2010. Absolute temperature change (top plots) and relative precipitation change (bottom plots), in winter (DJF) and summer (JJA).

6 Main contributions to the total variance

Figure 9 shows the contribution of RCM, GCM, scenario uncertainties and internal variability to the total variance for the near future (period 2021-2050). For temperature changes, GCM uncertainty is clearly the main contributor for both seasons, with more than 50% on oceans and seas. The second main contributor is the scenario uncertainty in the West and South of Europe in winter, and in the South and North of Europe in summer, for 25% to 50% of the total variance. RCM uncertainty is also important in summer over Central and Eastern Europe. On the contrary to temperature, for precipitation changes, the contribution of internal variability is large for the near future and exceeds 25% in many regions, especially in winter. For this temporal horizon, internal variability is therefore an important component. The contributions of GCMs and RCMs exhibit some clear patterns that are even more contrasted at the end of the century (see below).

Figure 10 now presents the different contributions to the total variance at the end of the century. For temperature, scenario uncertainty is by far the most important contributor. Its contribution exceeds 50% almost everywhere, except in the North-East of Europe and over the Norwegian Sea in winter, and over the Central Europe in summer. The other main contribution comes from the GCM uncertainty which presents a "hot-spot" over the Norwegian Sea, especially in winter. If negligible over oceans and seas where they are strongly constrained by the GCM fields, the contribution of the RCM uncertainty can be up to 35% over some continental areas (Central and Eastern Europe) in summer (see Table S15 of the SM). This enhanced summer role of RCMs is due to the larger contributions of local phenomena (convection) and feedbacks (soil moisture, cloud cover) to summer climate over the continental zones. It is noticeable that the RCM uncertainty is everywhere lower than 25% in winter. This probably means that, in winter, European climate change in temperature is mostly driven by large-scale advection imposed by the GCMs and that RCMs cannot really diverge from this large-scale influence.

For precipitation changes in 2071-2099, the largest contributions come from GCMs and RCMs in winter, followed by RCP scenarios. GCM uncertainty is by far dominant in the North-West of the domain. It is also very important over the Eastern Mediterranean Sea in winter. RCM uncertainty is important in many areas, namely over all continental areas in winter, and over almost the whole domain in summer. It is the largest contributor in the UK in winter, and in the North Sea in summer. The stronger role of RCMs in the total variance for precipitation, especially in summer, is related to a lower influence of the large-scale circulation imposed by the GCMs and a larger role of the RCM physical parameterizations and of the RCM soil moisture - atmosphere coupling to determine precipitation responses than for temperature. Scenario uncertainty is non-negligible in winter, over a rather large south-west toward north-east band: it reaches 35% in the North-East of Europe and can be greater than 50% around Morocco (see Table S13 of the SM). Except in some areas, summer precipitation projections are less sensitive to the scenario choice.

At the end of the century, internal variability is small, especially for temperature changes. It only exceeds 10% for precipitation changes over specific regions (e.g. South-West of Europe in winter, North Africa in summer). Note that the results of the uncertainty assessment can significantly depend on the method/hypotheses considered for the analysis. For instance, the internal variability variance and then its relative contribution to the total variance depend on the temporal and spatial aggregation scales considered for the studied variable. We choose here to estimate climate change for 30-year averages. The internal
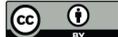
variability weight would have been much stronger for shorter temporal scales such as 20-year long periods as chosen in recent IPCC reports or even 10-year periods as in Hawkins and Sutton (2009).
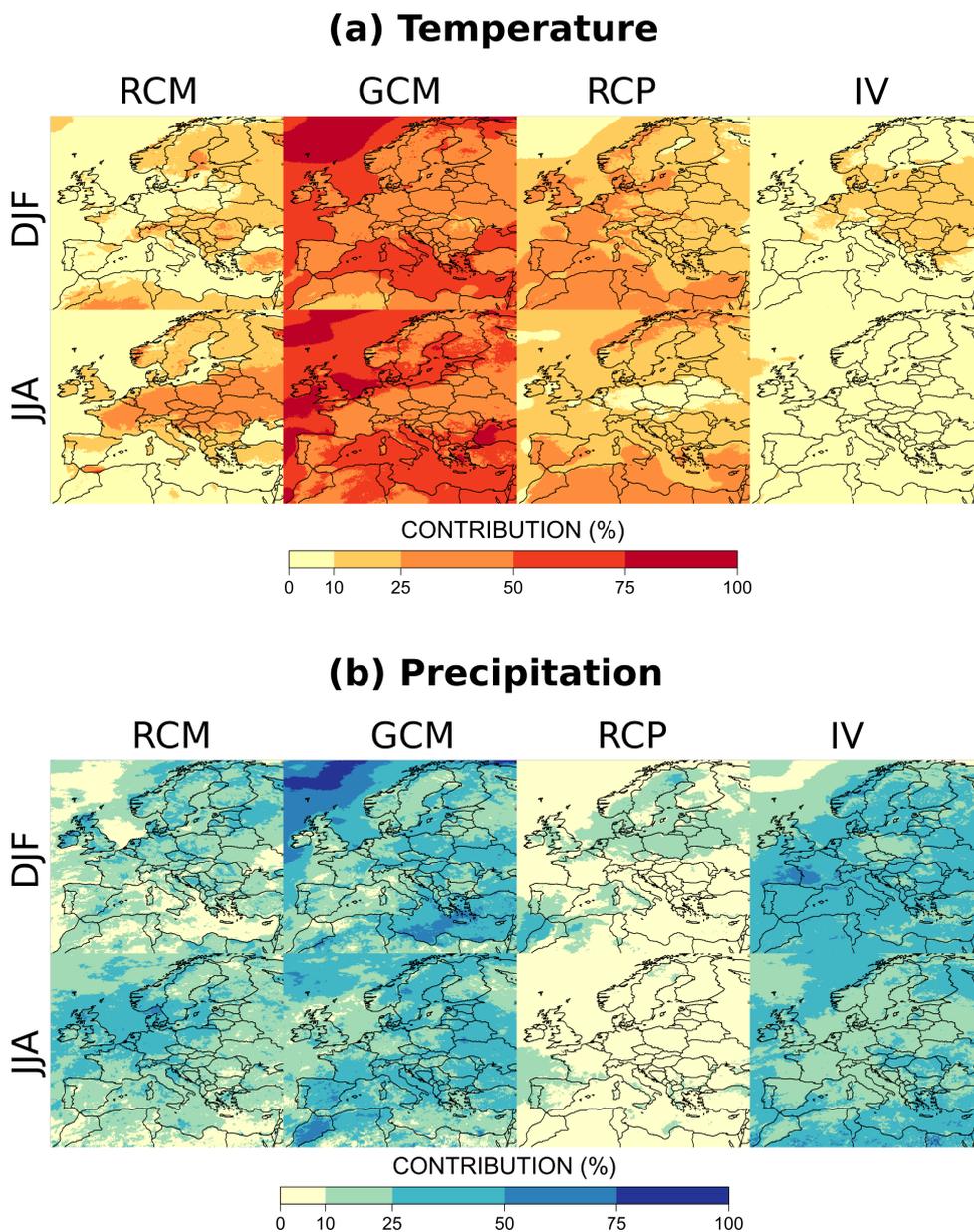
Figure 9. Fraction of total variance explained by the main sources of uncertainty: RCM, GCM, RCP scenario and internal variability (IV) for (a) absolute temperature changes and (b) relative precipitation changes, for the near future (2021-2050) compared to the period 1981-2010.

Figure S1 of the SM further provides the fraction of total variance explained by RCP/GCM, RCP/RCM and RCM/GCM interactions, and residual variability, for temperature and precipitation changes, in 2071-2099. These contributions are much
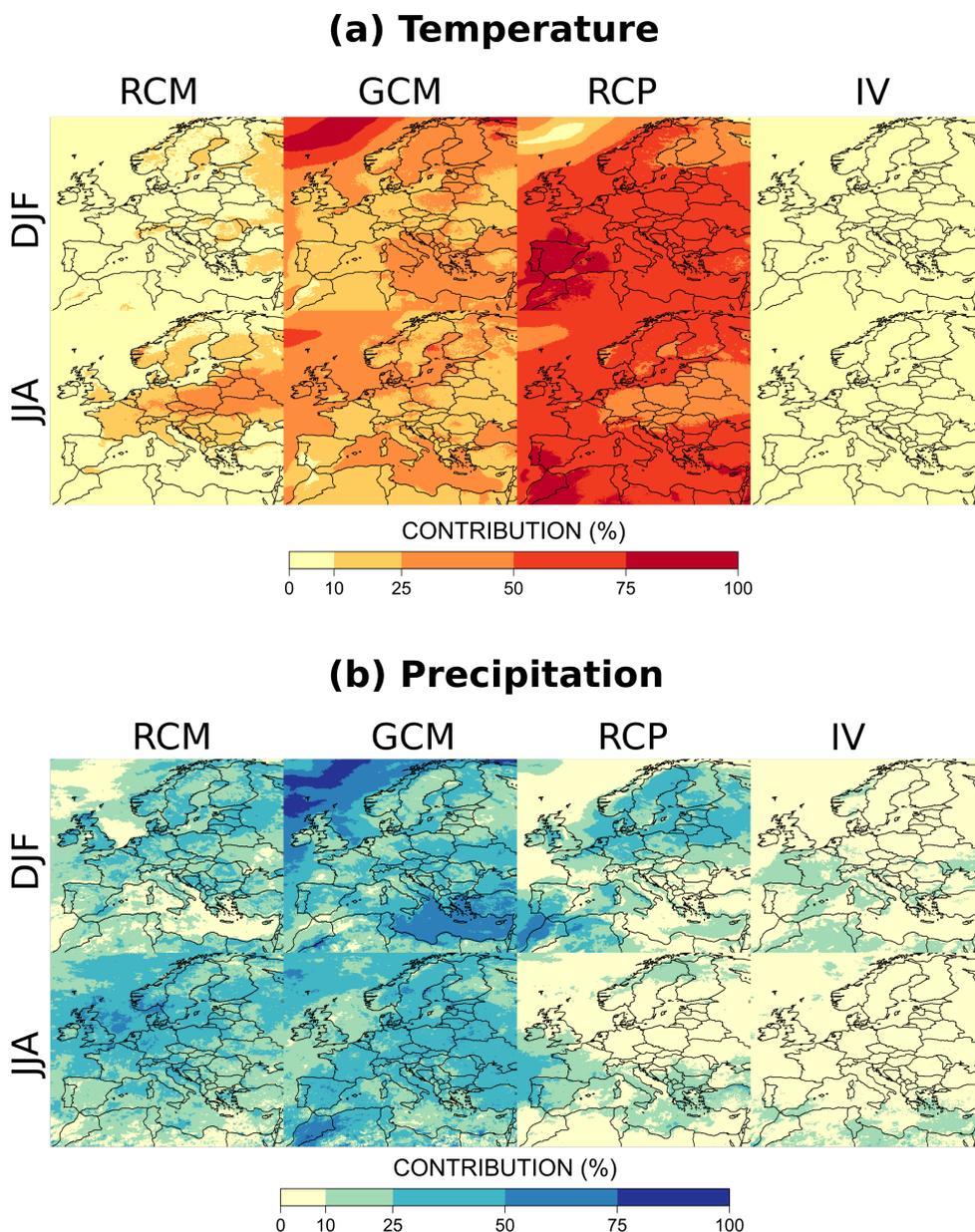
Figure 10. Fraction of total variance explained by the main sources of uncertainty: RCM, GCM, RCP scenario and internal variability (IV) for (a) absolute temperature changes and (b) relative precipitation changes, at the end of the twenty-first century (2071-2099) compared to the period 1981-2010.

310   smaller than the main sources (RCM, GCM, RCP scenario and internal variability). Residual variability and uncertainty due to the different interactions are all less than 5% for temperature changes, except in some small areas. For precipitation, moderate interactions (from 15% - 25%) are found for RCP/GCM interactions in winter, in Western Europe and Northern Italy, and

for RCM/GCM interactions in summer, in Southern Europe. Interactions between scenarios and RCMs are negligible, likely because RCP scenarios and RCMs are not directly connected inside the simulation chain. Residual variability is moderate, but
315 can contribute to more than 25% in summer, in some very dry areas. The main explanation for this result is the numerical instability of relative change estimates due to very low precipitation amounts during the reference period (see discussion in Section 8).

7 Individual contributions of each climate model

In this section, we focus on all GCMs and RCMs individually. For each GCM (resp. RCM), we consider the corresponding
effect (so-called main effect, i.e. the departure from the grand mean change for this specific GCM / RCM, in °C or %) and its
relative contribution to GCM uncertainty (resp. RCM uncertainty). Note that the main effects of all GCMs (resp. all RCMs)
sum to zero while individual relative contributions of all GCMs (resp. all RCMs) sum to one. Figure 11 shows the individual
contribution of each GCM to GCM uncertainty for temperature changes, as well as the main effect of each GCM, at the end
of the century. Clearly, GFDL-ESM2G has a strong influence in both seasons and leads to a lower warming than the others
(up to 2.5°C less in winter). In winter, HadGEM2-ES (Morocco, Spain) and IPSL-CM5A-MR (Scandinavia, Turkey) have also
important contributions in separate areas. CanESM2 has a strong influence in summer, particularly in the South of Europe.
Looking at the corresponding main effects, high discrepancies are obtained between some models. In winter, they can be up
to 5°C in North-Western Europe between GFDL-ESM2G and EC-EARTH or IPSL-CM5A-MR. In summer, CanESM2 leads
to a much higher warming almost everywhere (up to 2.5°C more than the mean climate change BM_k), this divergence being
particularly striking in the South of Europe.

Interpreting the results obtained for individual GCMs is not a simple task. The estimated temperature changes can be related
to the climate sensitivity of the models described in the Working Group I contribution to the IPCC's Fifth Assessment Report
(WGI AR5 IPCC, 2013). For instance, HadGEM2-ES and CanESM2 were considered to be very sensitive to the greenhouse
gases, being on the higher part of the CMIP5 range for the values of the Transient Climate Response (TCR) and of the
Equilibrium Climate Sensitivity (ECS). As indicated in the last IPCC report (AR6, chapter 7), HadGEM2-ES and CanESM2
have a TCR (resp. ECS) equal to 2.38°C (3.96°C) and 2.37°C (3.71°C), that is to say near the 95% percentile value of the
total CMIP5 TCR or ECS ranges. As RCMs tend to follow their driving GCMs for temperature change, they logically lead to
a larger warming over Europe when used as RCM drivers. On the contrary, GFDL-ESM2G lies on the lower part of the TCR
and ECS IPCC ranges (0.96°C and 2.3°C respectively) and logically leads to a weaker warming in the RCMs driven by it.

For precipitation changes (see Fig. 12), the GCMs CanESM2, CNRM-CM5, IPSL-CM5A-MR and EC-EARTH show the
most important contributions to GCM uncertainty. We recall here that the sum of the GCM (resp. RCM) main effects is equal to
zero and that changes shared by all GCMs (resp. RCMs) correspond to the mean change of the ensemble. In winter, in compar-
ison to all the other GCMs, IPSL-CM5A-MR leads to greater winter precipitation changes in Northern Europe. For the same
season, the wetter EC-EARTH and the dryer GFDL-ESM2G and MIROC5 GCMs lead to a "hot-spot" of uncertainty in the far
North-West highlighted in Fig. 10. In summer, CanESM2 simulates over almost the whole domain much less precipitation than
the other GCMs. For precipitation changes, the interpretation of individual GCM contributions is more complicated because
the GCM global climate sensitivity is not very informative and the RCMs can diverge more from the climate change pattern of
their driving GCM. However, these spatial patterns are globally in line with previous studies (see discussion in Section 8).

Similarly, Figures 13 and 14 present the individual contributions of the different RCMs to RCM uncertainty, for temperature
and precipitation changes, respectively. For winter temperature, HadREM3-GA7 and REMO are warming much more than
the other RCMs in the North-East of Europe (up to 2°C more than the average behaviour). This feature is compensated in

the ensemble by a more moderate warming provided by ALARO-0 and ALADIN63, both being from the same model family. At a smaller scale, RCA4 shows a striking warming over the Alps and the Carpathians mountain range. This explains the large contribution of RCA4 to the RCM uncertainty there and can likely be explained by an abnormal snow cover response to

355 warming as discussed for example in Fernández et al. (2019), even though for a different season and temporal horizon.

For summer temperature, HadREM3-GA7 shows a striking feature being 2.5°C warmer than the multi-model average over the whole continental Europe. To our knowledge, this model is intercompared here for the first time within the EURO-CORDEX context and this behaviour is not reported so far in the literature. As a potential explanation, we can only say that HadREM3-GA7 is probably very sensitive to anthropogenic forcings as is HADGEM2-ES, the Hadley Center applying

360 a seamless approach across its model hierarchy. On the contrary, WRF381P is warming less than the other RCMs over Western Europe (up to -1.5°C), explaining its strong individual contribution to the RCM uncertainty over the area. Except for RACMO22E, it is also worth mentioning that the RCMs taking into account evolving aerosol forcing along the projection simulations (Gutiérrez et al., 2020) are generally warming more that the other RCMs in summer (ALADIN53, ALADIN63, ALARO-0, HadREM3-GA7). This behaviour is well aligned with results obtained by Boé et al. (2020). Indeed, as anthro-

365 pogenic aerosols are declining during the 21st century, their dimming effect is also decreasing, leading to an increase in surface solar radiation and potentially an enhanced warming with respect to RCMs which do not take this effect into account.

Finally, for temperature changes, many RCMs (ALADIN53 and CCLM4-8-17 in winter, WRF381P and WRF361H for both seasons) show noticeable behaviours over oceanic areas (Baltic Sea, North Atlantic, Mediterranean Sea, the Channel), the corresponding main effects being however moderate. This feature is not expected in RCMs as the 2-meter temperature over

370 the sea is largely imposed by the driving GCM SST and should be similar in all RCMs driven by the same SST field. For ALADIN53, this is likely the signature of a known issue in the way to force the SST from the driving model.

For winter precipitation (see Fig. 14), WRF361H, HadREM3-GA7 and COSMO-crCLIM produce smaller total precipitation than the other RCMs, respectively over Central-North Europe, North Atlantic and North Africa. At the opposite ALADIN53, ALADIN63, RegCM4-6 and HIRHAM5 show more local spots where projected precipitation amounts are higher than the

375 mean change. For summer precipitation, the influential models are neither the same nor over the same areas. WRF381P has a clear wetter (or less dry) signal than the ensemble over a large part of the domain. At the contrary, HadREM3-GA7 is largely drier than the average for the whole Northern Europe as is WRF361H for the North Atlantic part of the domain.

The most influential RCMs are thus easily identified. Locally, one RCM can often explain more than 50% of the RCM uncertainty range. We can cite for example HadREM3-GA7 and WRF381P for summer temperature and precipitation, WRF361H

380 for precipitation in both seasons and ALADIN53 and RACMO22E more locally for winter temperature. Such high values in the RCM individual contributions may guide future investigations in order to understand those specific model behaviours and to verify if the RCM uncertainty range is not artificially too large due to modelling issues. On the contrary, RCA4 seems to be the only RCM that generally weakly influences the ensemble behaviour. Its individual contribution is nearly always below 20% except very locally for the Alps and the Carpathians for winter temperature and the Channel for summer temperature.
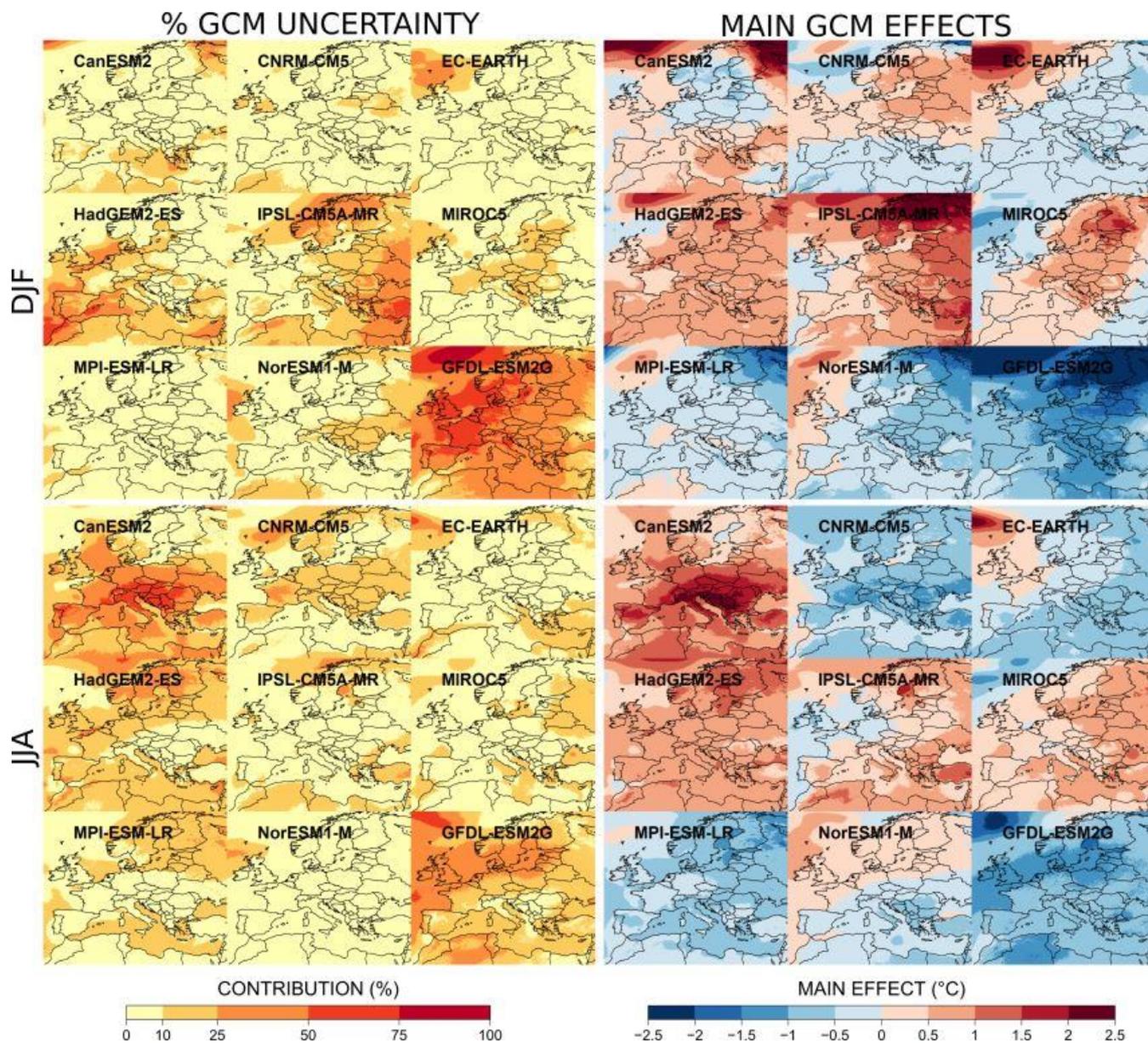
Figure 11. Fraction of GCM uncertainty (left plots) and main GCM effects (right plots) for each GCM, for absolute temperature changes in winter (DJF) and summer (JJA), at the end of the twenty-first century (2071-2099) compared to the period 1981-2010.
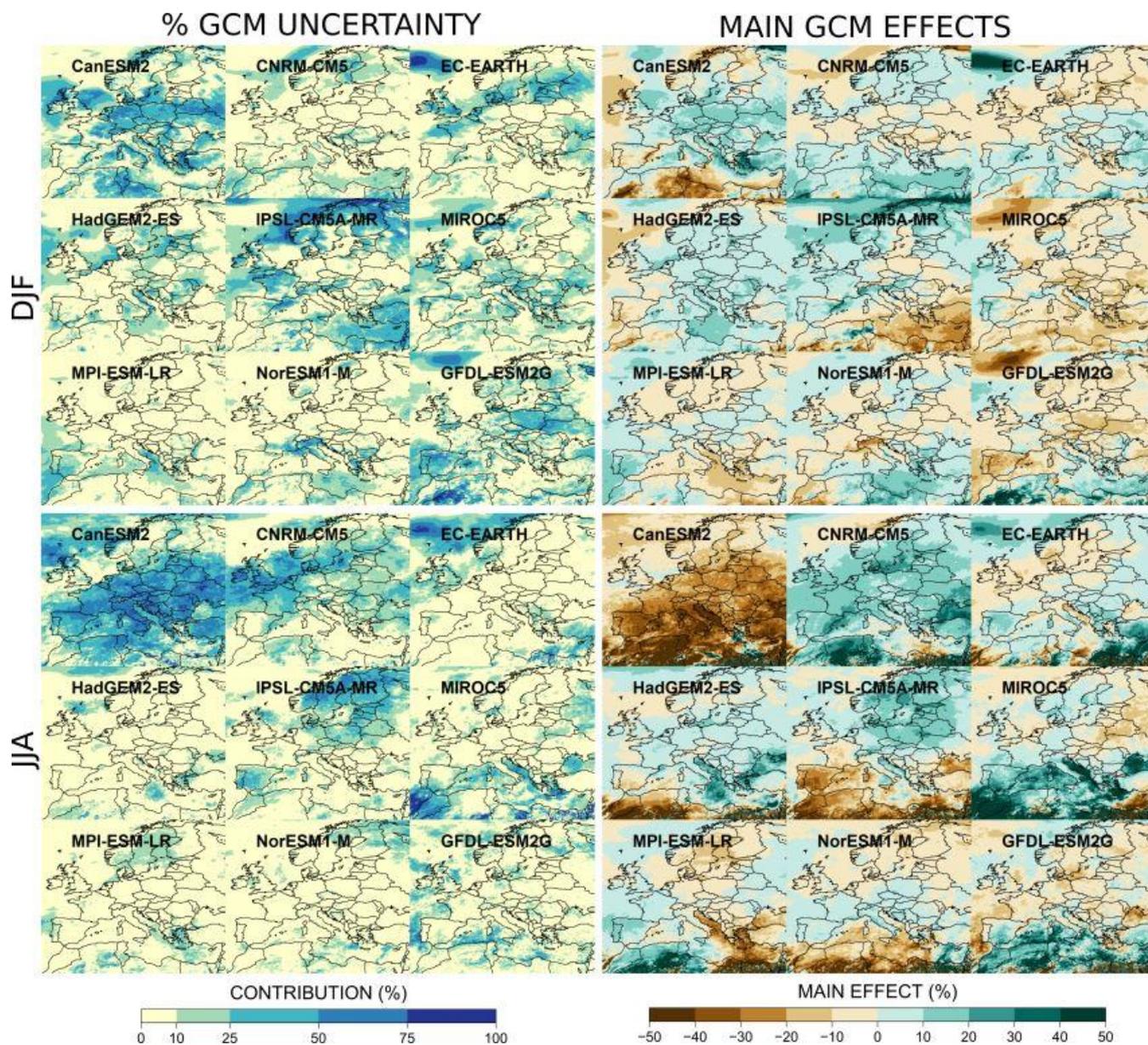
Figure 12. Fraction of GCM uncertainty (left plots) and main GCM effects (right plots) for each GCM, for relative precipitation changes in winter (DJF) and summer (JJA), at the end of the twenty-first century (2071-2099) compared to the period 1981-2010.
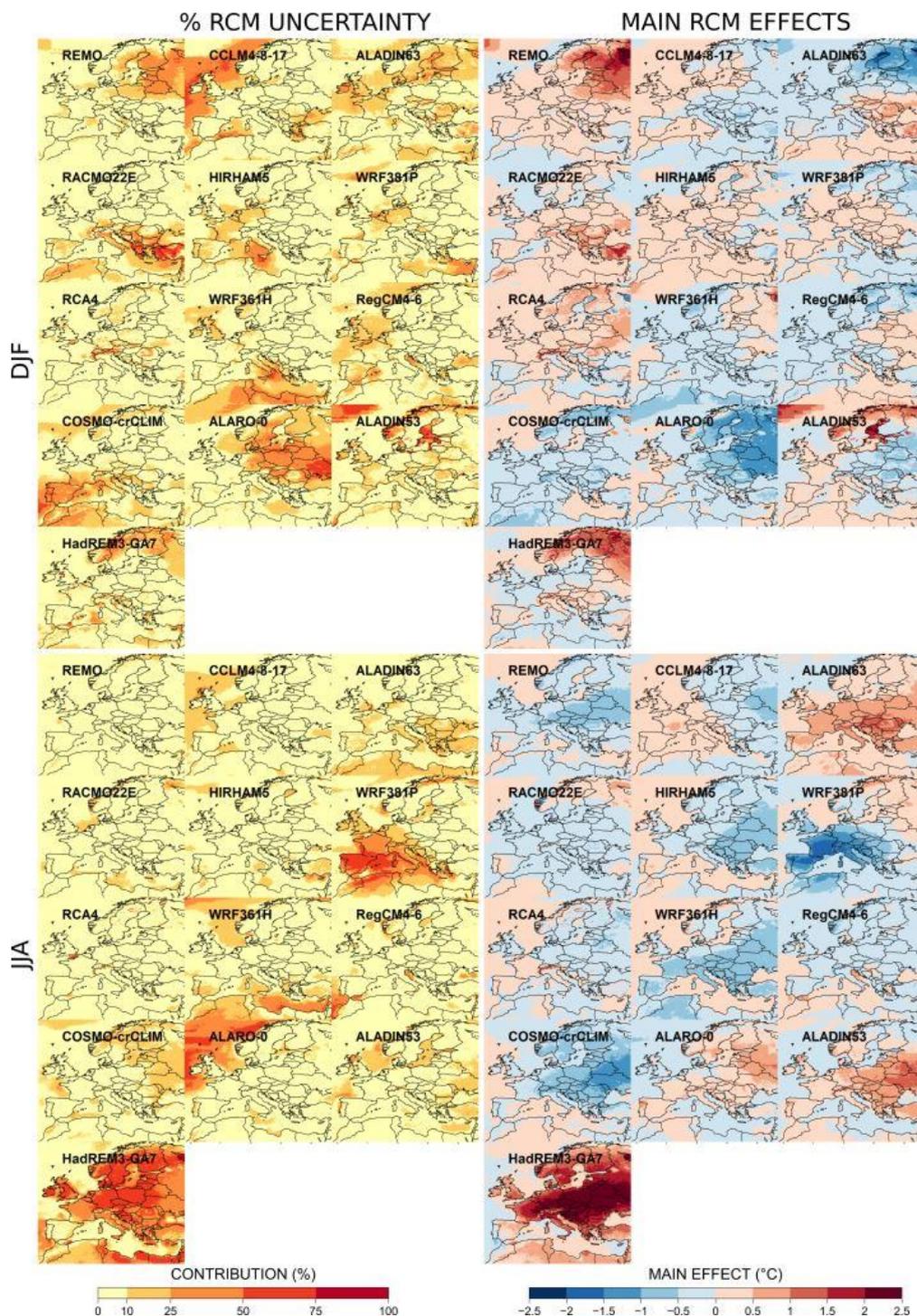
Figure 13. Fraction of RCM uncertainty (left plots) and main RCM effects (right plots) for each RCM, for absolute temperature changes in winter (DJF) and summer (JJA), at the end of the twenty-first century (2071-2099) compared to the period 1981-2010.
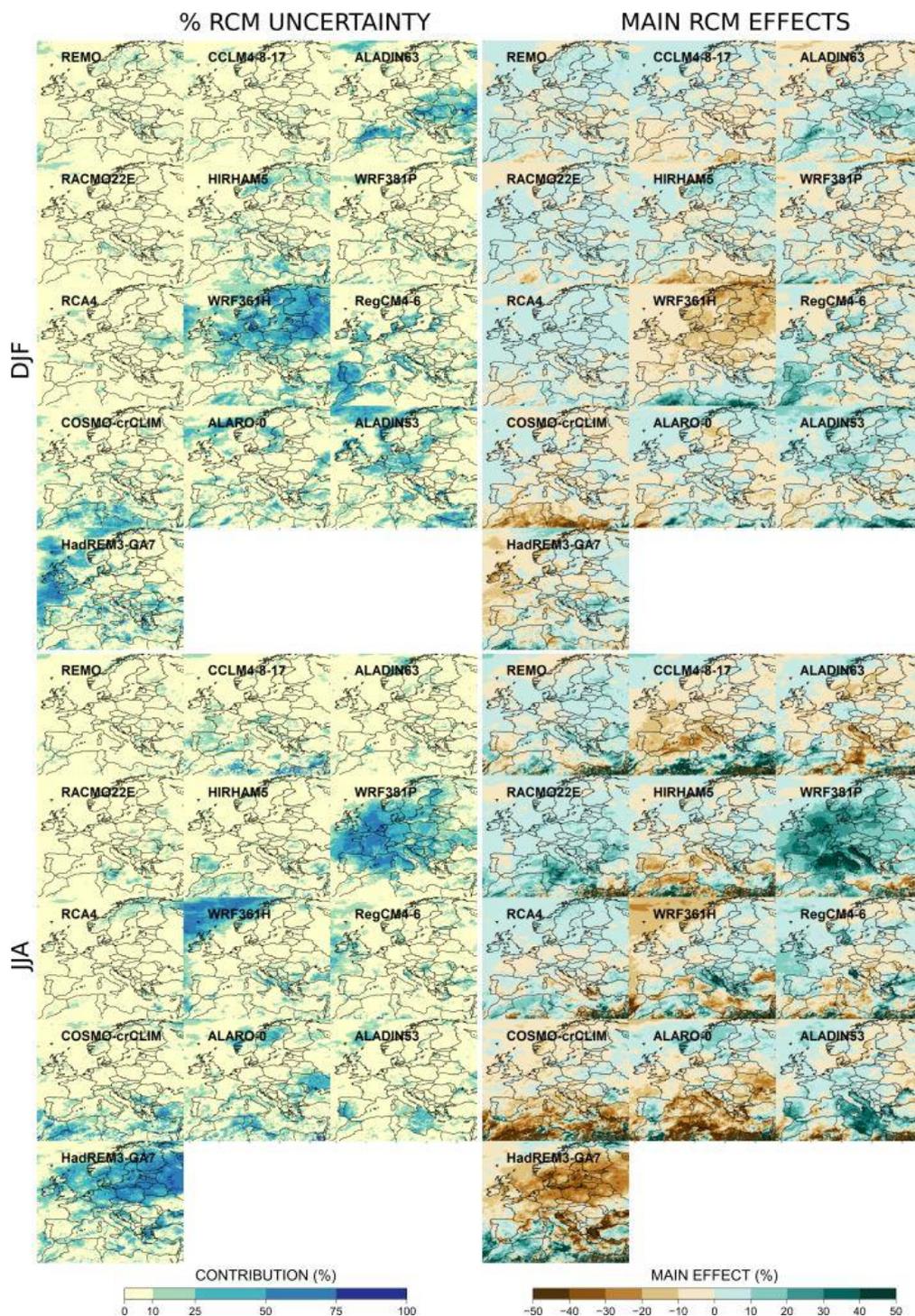
Figure 14. Fraction of RCM uncertainty (left plots) and main RCM effects (right plots) for each RCM, for relative precipitation changes in winter (DJF) and summer (JJA), at the end of the twenty-first century (2071-2099) compared to the period 1981-2010.

8 Discussion

8.1 Unbalanced MMEs: influence of the statistical approach

The projected mean change of any climate variable is typically estimated with the direct average of the climate change responses obtained for the different simulations of the available ensemble (see, e.g. Jacob et al., 2014; Fernández et al., 2019; Coppola et al., 2020; Vautard et al., 2020). Direct averages are however likely to be poor estimates of mean changes in the case of unbalanced and/or incomplete ensembles. As motivated by several papers (Déqué et al., 2007, 2012; Northrop and Chandler, 2014; Evin et al., 2019), a proper statistical treatment of unbalanced ensembles is important in order to exploit ensembles of opportunity and avoid unrepresentative estimates of the mean projected changes or even of the likely range. For each scenario k, Figure 15 shows the differences between the balanced mean climate change response BM_k obtained with the QUALYPSO approach and the direct average M_k of the climate change responses available for each scenario. In summer, important differences can be observed, in particular for temperature changes in Eastern Europe with the RCP2.6 and RCP4.5 (the balanced estimate is up to 0.8°C warmer) and for precipitation changes with the RCP4.5 (the balanced estimate is drier than the direct average by up to 20% in Eastern Europe). The winter season is also affected with a balanced estimate that indicates a weaker warming than the direct average, by up to 0.5°C (see, e.g. Central and Northern Europe for the RCP8.5).

The very unbalanced nature of available MMEs is thus an important issue that should not be overlooked. The most critical configurations correspond to unbalanced ensembles where the less consensual and/or the most different GCMs/RCMs (as expressed from the spatial signatures of their main effects) are under-represented, which is the case in this study. Indeed, the GCM CanESM2 and RCM HadREM3-GA7 clearly stand out from the other climate models (see Figs. 11-13) whereas they only participate to 2 and 1 simulation chains among the 87 members of our ensemble, respectively. In this case, the direct average of the MME is thus a misleading estimate of the mean projected changes and differs greatly from the estimate that we would obtain with a balanced MME.

8.2 Comparison to previous works

The results shown in this study can be compared to previous studies aiming at estimating mean future changes and partitioning the different sources of uncertainties in EURO-CORDEX ensembles.

8.2.1 Mean future changes: importance of the MME configuration and of the experiment

It is worth mentioning that numerous parameters and configurations can impact the estimates of mean future changes. As shown above, some climate models included in the analysis can greatly influence the obtained mean projected changes and related uncertainties. This result is somewhat in contradiction with the study by Fernández et al. (2019) which concludes to a moderate influence of the subsampling, though this study is performed over a small region (around Spain), for the near future only (2021-2050) and for a smaller diversity of RCMs and GCMs (9 RCMs and 8 GCMs at a 0.11° resolution). Projected changes are also

415 strongly dependent of the experiment and of the different versions of the climate models. For example, the study by Coppola et al. (2020) notices much stronger projected changes with the recent CMIP6 MME than with the EURO-CORDEX MME.

In this study, the seasonal mean temperature and total precipitation changes at the end of the century (Fig. 7) obtained with the RCP8.5 scenario can be compared to Figures 1 and 5 in Coppola et al. (2020). The spatial patterns of these changes are obviously very similar (a larger projected warming in the North and Northeast of Europe in winter, in the South in summer,

420 positive precipitation changes in the Northern part and negative changes in the Southern part, with a different zero-change line in winter and summer). It is difficult to have a precise comparison considering the different color scales, but different factors could explain potential differences. First, the MME considered in this study is larger than in Coppola et al. (2020), with one more GCM (GFDL-ESM2) and two more RCMs (ALARO-0 and HadREM3-GA7) having strong influence on mean temperature changes in winter (GFDL-ESM2 and ALARO-0) and summer (HadREM3-GA7) and summer precipitation changes

425 (HadREM3-GA7). Secondly, as discussed above, the method of estimation (i.e. balanced versus direct estimates) also impacts estimates of mean projected changes, though it is difficult to quantify in comparison to Coppola et al. (2020) due to the different MME.

8.2.2 Contribution of the main sources of uncertainty

This study emphasizes the main sources of uncertainty over Europe (Figs. 9-10). GCM uncertainty overcomes RCM uncer-

430 tainty for temperature, even if RCM uncertainty can contribute to 25%-50% in summer, over continental Europe. These results are in agreement with Christensen and Kjellström (2020) (see their Fig. 5) who also find a moderate contribution of RCMs for winter temperature, except in several regions (e.g. Turkey, over the Alps), where small contributions are also shown in this study. The remarkable "hot-spot" of uncertainty in the North-West of Europe, due to disagreements between the GCMs, is also clearly visible in their study. For summer temperature, a noticeable difference is the small contribution of RCMs over

435 continental Europe, largely smaller than for GCMs while our study exhibits an important contribution (more than 25%) in Eastern Europe, surpassing GCM contribution. This can be easily explains by the much larger set of RCMs used in our study, important contributors of the RCM uncertainty (HadREM3-GA7, ALARO-0, WRF386P, WRF361H) being absent in Christensen and Kjellström (2020). Conclusions are globally similar for precipitation changes, GCM and RCM contributions being both important in winter and summer. The GCM contribution is also usually greater than RCM contribution in Christensen

440 and Kjellström (2020), and almost equivalent in summer, this result being shared by the study of Déqué et al. (2012) (see their Fig. 1). Unsurprisingly, scenario uncertainty is more important at the end of the century (2071-2099) than for the near future (2021-2050). At the end of the century, scenario uncertainty overcomes the other sources of uncertainty for temperature changes (generally more than 50%), while its contribution is more moderate for precipitation changes, especially in summer (less than 25% and often less than 10%), corroborating previous studies by Hawkins and Sutton (2009); Déqué et al. (2012).

445 ### 8.2.3 Contribution of individual GCMs and RCMs

For individual GCM/RCM contributions, the results shown in this study can be compared to the outcomes of McSweeney et al. (2015) who analyse the climate change signal of individual CMIP5 GCMs over Europe in winter and summer at the end of

the 21st century under the RCP8.5 scenario. Our results are in full agreement with their results. For the GCMs used in EURO-CORDEX, they find that HadGEM2-ES (resp. GFDL-ESM2G and NorESM1-M) is the GCM that warms the most (resp. the less) in winter over Europe and that HadGEM2-ES and CanESM2 (resp. GFDL-ESM2G, CNRM-CM5 and MPI-ESM-LR) are the GCMs that warm the most (resp. the less) in summer. In addition, considering the projected precipitation increase over most of continental Europe in winter, they also indicate that MIROC5 and GFDL-ESM2G are among the CMIP5 GCMs simulating the weakest wettening whereas HadGEM2-ES and CanESM2 are the EURO-CORDEX-used GCMs simulating the largest precipitation increase for this season. In summer, while mean projected changes exhibit a decrease in precipitation changes in the Western and Southern Europe, individual GCM patterns are strongly contrasted, CNRM-CM5 showing a strong wettening compared to the other GCMs for example, while CanESM2 is particularly drier. Note however that CanESM2 is not identified as particularly drying in summer in McSweeney et al. (2015). Re-assessing the CanESM2/REMO and CanESM2/CCLM4-8-17 simulations could help understanding and identifying a potential GCM-RCM inconsistency. The "hot-spot" of GCM uncertainty in the North-West of the domain over the North-Atlantic ocean is likely related to the sea ice cover change in particular in winter. A precise interpretation is difficult to obtain using the current literature but it is worth underlining that two of the GCMs showing a strong influence in this area (CanESM2, IPSL-CM5A-MR) are considered among the most trustable CMIP5 GCMs concerning the wintertime sea ice cover. MIROC5, NorESM1-M and CNRM-CM5 are however mentioned as strongly biased for the Arctic sea ice cover in winter (Stroeve et al., 2012), the other driving GCMs are not analyzed in the study. In future EURO-CORDEX multi-model initiative, it is therefore advised to evaluate the sea ice cover extent of the potential driving GCMs before selecting them (Stroeve et al., 2012).

Besides, Zappa and Shepherd (2017) propose four contrasted storylines for projected wintertime Mediterranean precipitation changes. They classify GFDL-ESM2G in the model family leading to the strongest decline whereas EC-EARTH, HADGEM2-ES and NorESM1-M belong to the family of the weakest decline or wettening for the region in winter (personal communication). Contrary to McSweeney et al. (2015), the classification proposed by Zappa and Shepherd (2017), though very relevant, does not help to understand our findings for precipitation changes.

Except for the evolving aerosol effect described in section 7, it is difficult so far to explain the RCM individual behaviour as the most influencing RCMs of the current study have not always been included or detected in previous articles dealing with EURO-CORDEX projections (e.g. Sørland et al., 2018; Fernández et al., 2019; Boé et al., 2020; Christensen and Kjellström, 2020). We consider however that the identification of strong RCM individual effects in our study motivates the definition of a standardized indicator of regional climate model sensitivity mimicking the ECS or TCR indicators for GCMs.

8.2.4 Internal variability

This study highlights the small contribution of internal variability at the end of the century, for both temperature and precipitation changes, though internal variability can reach more than 10% in some areas for winter precipitation changes (e.g. Mediterranean region, see Table S13 in the SM). As discussed in Section 6 and shown in Hawkins and Sutton (2009), the temporal and spatial resolution (0.11° pixel, country, SREX region) greatly influences internal variability. A larger contribu-

tion would have been obtained with a smaller temporal window (e.g. using 20-year long periods as in recent IPCC reports or 10-year periods as in Hawkins and Sutton (2009)).

8.2.5 Interactions

Finally, in this study, the different paired interactions between RCP scenarios, GCMs and RCMs are shown to be negligible
485   for temperature changes, and for RCP/RCM interactions. For precipitation changes, however, RCP/GCM interactions can contribute to more than 20% in some areas in winter (along the coastlines of France, Spain and Portugal, over the Alps) and for RCM/GCM interactions, particularly in summer. Christensen and Kjellström (2020) share these results (see their Fig. S14), RCM/GCM interactions contributing to 5%-20% of the total variance for summer precipitation over all Europe and the Mediterranean sea.

490   ### 8.3 Significance of the mean changes

A recurrent question related to the assessment of changes is their statistical significance. Many studies rely on standard statistical tests. They are used for instance to assess the significance of the trend (e.g. Mann-Whitney-Wilcoxon test Jacob et al., 2014) or Student t-test (Christensen et al., 2019) for each simulation chain, test the significance of signal-to-noise ratios when multiple replicates of a same chain are available (e.g. t-tests of WRF simulations in Laux et al., 2017), test the significance of
495   the components of an ANOVA decomposition (e.g. F-test in Christensen and Kjellström, 2020).

In the present study, we focus on mean changes BM_k estimated from the whole MME (and not individual climate change responses), and put them in relation to the uncertainty BU. In this perspective, as recommended by von Storch and Zwiers (2013), we do not rely on a statistical significance test for the following reasons:

- statistical testing relies on strong assumptions that are often doubtful in the case of large ensembles of climate simu-
500   lations. For example, the independence of the replicates can be put into question for RCM outputs forced by the same GCM simulation. Similarly, it is difficult to assume that the climate variables obtained from different simulation chains have similar distributional properties.

- Even if statistical testing is completely appropriate, the dependency of the power of statistical tests on the number of simulation chains remains a strong limitation for their interpretation.

505   - Statistical tests require a sample representative of a "population" describing the whole set of possible values. In the context of testing ensemble of climate change scenarios, the definition of this population is unclear (all climate scenarios? All available climate scenarios? Climate scenarios based on a specific emission scenario and produced with a restricted class of models?).

In this study, we compare the absolute ratio $|BM_k/BU|$ to one in order to assess if mean projected changes are greater than
510   the corresponding uncertainty, this simple approach having the advantage to have a direct interpretation.

8.4 Limitations and technical difficulties

This study applies the QUALYPSO methodology described in Evin et al. (2019) which implies data augmentation and a Bayesian approach to augment the RCP/GCM/RCM matrix and properly treat unbalanced ensembles, and estimate the main RCP, GCM and RCM effects. Due to the high number of missing quantities to be inferred, the estimation of interactions us-
515 ing QUALYPSO is not feasible, and we resort to heuristic estimates of some interaction effects (i.e. when at least 2 runs are available to estimate this interaction). As an alternative, Northrop and Chandler (2014), using a random-effect approach and a Bayesian implementation, propose to directly infer the variability (i.e. standard deviation) between the RCPs, GCMs and between RCP/GCM interactions. Instead of trying to infer all individual effects (for which few or no runs may be available), their approach directly tackles the partition of the different uncertainties in unbalanced MMEs. However, contrary to QUALYPSO,
520 their approach does not provide estimates of individual GCM or RCM effects. As shown in this study, individual contributions of specific GCMs or RCMs are interesting to assess since, as discussed above, they can guide future investigations.

A major technical difficulty is related to the computation of relative precipitation change in dry areas. Indeed, for some regions (typically the middle-east), the average summer precipitation is very low for the reference periods. As a consequence, the ratio between future and reference periods is numerically unstable and can be huge for some simulation chains. As can be
525 seen in Table S17 of the SM, in these situations, the uncertainty can be huge (see, e.g. BU obtained for precipitation changes equals to 242% and 392% for Cairo, Egypt and Damascus, Syria, respectively). For these regions, large changes in relative terms correspond actually to small changes in absolute values (see also Bichet et al., 2020, for an application of QUALYPSO to relative and absolute precipitation changes in Africa) such that absolute precipitation changes are actually more meaningful.
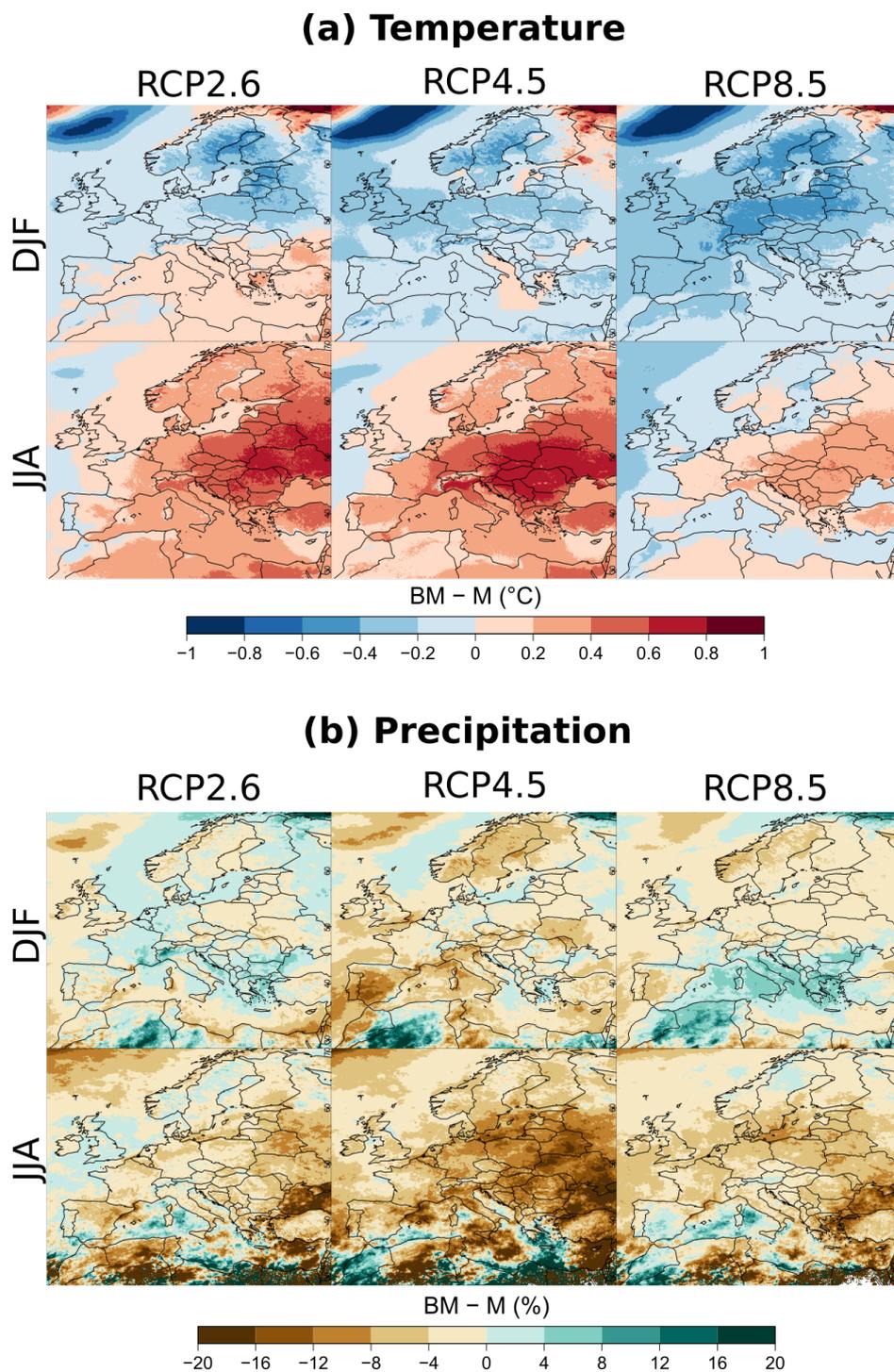
Figure 15. Difference between the "balanced" estimates of the mean projected changes BM_k obtained with the QUALYPSO approach and the direct average M_k of the climate change responses available for each scenario in winter (DJF) and summer (JJA), at the end of the twenty-first century (2071-2099) compared to the period 1981-2010 for mean projected changes of (a) precipitation (b) temperature.

9   Conclusion

530   This paper proposes a thorough assessment of mean climate change responses and related uncertainties over Europe, for mean
seasonal temperature and total seasonal precipitation. QUALYPSO, an advanced statistical approach based on an ANOVA
method and data augmentation, is applied to a large MME of 87 high-resolution (0.11°) EURO-CORDEX projections. QUA-
LYPSO provides a balanced estimate of all the parameters of the analysis, including the mean climate change signal and the
associated uncertainty components. For the first time, we provide a comprehensive estimation of the relative contribution of
535   GCM and RCM climate models, of RCP scenarios and of internal variability to the total variance of the largest ensemble
publicly available up-to date [1].

For temperature, RCP uncertainty is the most important contributor at the end of the century, particularly on lands, but
GCM uncertainty is also important on seas and on the Atlantic ocean and RCM contribution reaches 30% in Central Europe in
summer. For precipitation, GCM and RCM uncertainties are the most important contributors to the total variance in summer at
540   the end of the century, while scenario uncertainty also plays a major role in winter. GCM uncertainties are more important in
the Norwegian Sea and over the Eastern part of the Mediterranean sea in winter, while RCM uncertainties can be dominant in
some specific regions (e.g. between UK and Germany in summer). A strong contrast between lands and seas/oceans can also
be noticed for summer temperature changes and winter precipitation changes.

In this study, internal variability is small compared to the other sources of uncertainty. As 30-year averages of the simulation
545   chains are taken, most of the high-frequency variability is removed, and the low-frequency part only is usually negligible in
comparison of the dispersion between the GCMs/RCMs. The residual variability and the different interactions are also shown
to be usually small in our analyses, compared to the other sources of uncertainties, the most noticeable interactions being
observed for precipitation changes, namely RCP/GCM interactions in winter and GCM/RCM interactions in summer.

For each major source of uncertainty, we also identify individual GCM and RCM models explaining the greatest part of the
550   corresponding uncertainty. The large values of uncertainty components are produced by a few "outlier" models in the sense
that they strongly depart from the average of the MME. The legitimacy of this divergence must then be questioned. Are there
strong reasons to discard this particular model (bugs, wrong parameterizations or model structures, etc.)? In that case, it seems
reasonable to omit these climate models from the MMEs. Otherwise, the inclusion of these models is crucial in order to avoid
an underestimation of the uncertainty.

555   A critical issue is finally related to the very unbalanced and incomplete nature of ensembles of opportunity. The over/under
representation of some RCM and GCM models forbids the application of standard ANOVA methods and the estimation of
the mean changes by direct averages of these ensembles. In most past studies, changes are estimated from the average of all
simulations (Jacob et al., 2014; Coppola et al., 2020). We show here that the average can be a poor estimate of the mean
projected changes. The difference between a direct average and a "balanced" estimate is likely to increase with the unbalanced
560   level of the MME and can be dramatically large when the under-represented models are atypical. In the present case, we show
that the projected warming could be up to 0.8°C larger than previously estimated by the end of the century for RCP2.6 and

---

[1]on Aug. 2020

RCP4.5 over large parts of central Europe in summer. On the contrary, the projected warming can be up to 0.4°C smaller in winter in Northern Europe. Using a balanced estimate, the decrease of summer precipitation by the end of the century can be up to 20% larger in Central-Eastern Europe for RCP4.5.

565   This work urges the community (1) to develop new strategies for future multi-model initiatives based on regional climate models, in particular by carefully selecting plausible GCMs and RCMs and by favouring their diversity in terms of climate change response at regional scale and cover at best the plausible futures, (2) to choose MME in close collaboration with statistician specialists in order to envisage the best way to "fill" or "balance" the ensembles a posteriori and (3) to adopt robust and appropriate statistical methods for the assessment and usage of large available MMEs. The purpose of these advises

570   is to improve the reliability of the regional climate change information provided to the scientific communities as well as to various climate data users through climate services. There is a critical need for the development of best practices dedicated to the dissemination of results based on large ensembles of climate projections, at the destination of the managers/practitioners, which include not only climate scientists, but also geophysical and data scientists.

Acknowledgments

575   This work was partly supported by the French National program LEFE (Les Enveloppes Fluides et l'Environnement). S. Somot has been partly supported by the EUCP and C3S_34b_lot2 projects. EUCP is financed by the European Commission through the Horizon 2020 Programme for Research and Innovation, Grant Agreement 776613. C3S_34b_lot2 is funded by the Copernicus Climate Change Service. ECMWF implements this service on behalf of the European Commission. We thank the CMIP5 and EURO-CORDEX modelling groups for freely providing the simulations used in this study.

References

Bichet, A., Diedhiou, A., Hingray, B., Evin, G., Touré, N. E., Browne, K. N. A., and Kouadio, K. (2020). Assessing uncertainties in the regional projections of precipitation in CORDEX-AFRICA. *Climatic Change*.

Boé, J., Somot, S., Corre, L., and Nabat, P. (2020). Large discrepancies in summer climate change over Europe as projected by global and regional climate models: causes and consequences. *Climate Dynamics*, 54(5):2981–3002.

Christensen, J. H., Larsen, M. A. D., Christensen, O. B., Drews, M., and Stendel, M. (2019). Robustness of European climate projections from dynamical downscaling. *Climate Dynamics*, 53(7):4857–4869.

Christensen, O. B. and Kjellström, E. (2020). Partitioning uncertainty components of mean climate and climate change in a large ensemble of European regional climate model projections. *Climate Dynamics*.

Coppola, E., Nogherotto, R., Ciarlò, J. M., Giorgi, F., Meijgaard, E. v., Kadygrov, N., Iles, C., Corre, L., Sandstad, M., Somot, S., Nabat, P., Vautard, R., Levavasseur, G., Schwingshackl, C., Sillmann, J., Kjellström, E., Nikulin, G., Aalbers, E., Lenderink, G., Christensen, O. B., Boberg, F., Sørland, S. L., Demory, M.-E., Bülow, K., Teichmann, C., Warrach-Sagi, K., and Wulfmeyer, V. (2020). Assessment of the European climate projections as simulated by the large EURO-CORDEX regional and global climate model ensemble. *Journal of Geophysical Research: Atmospheres*, 125:e2019JD032356.

Déqué, M., Rowell, D. P., Lüthi, D., Giorgi, F., Christensen, J. H., Rockel, B., Jacob, D., Kjellström, E., Castro, M. d., and Hurk, B. v. d. (2007). An intercomparison of regional climate simulations for Europe: assessing uncertainties in model projections. *Climatic Change*, 81(1):53–70.

Déqué, M., Somot, S., Sanchez-Gomez, E., Goodess, C. M., Jacob, D., Lenderink, G., and Christensen, O. B. (2012). The spread amongst ENSEMBLES regional scenarios: regional climate models, driving general circulation models and interannual variability. *Climate Dynamics*, 38(5):951–964.

Evin, G., Hingray, B., Blanchet, J., Eckert, N., Morin, S., and Verfaillie, D. (2019). Partitioning Uncertainty Components of an Incomplete Ensemble of Climate Projections Using Data Augmentation. *Journal of Climate*, 32(8):2423–2440.

Fantini, A., Raffaele, F., Torma, C., Bacer, S., Coppola, E., Giorgi, F., Ahrens, B., Dubois, C., Sanchez, E., and Verdecchia, M. (2018). Assessment of multiple daily precipitation statistics in ERA-Interim driven Med-CORDEX and EURO-CORDEX experiments against high resolution observations. *Climate Dynamics*, 51(3):877–900.

Fernández, J., Frías, M. D., Cabos, W. D., Cofiño, A. S., Domínguez, M., Fita, L., Gaertner, M. A., García-Díez, M., Gutiérrez, J. M., Jiménez-Guerrero, P., Liguori, G., Montávez, J. P., Romera, R., and Sánchez, E. (2019). Consistency of climate change projections from multiple global and regional model intercomparison projects. *Climate Dynamics*, 52(1):1139–1156.

Gao, X., Pal, J. S., and Giorgi, F. (2006). Projected changes in mean and extreme precipitation over the Mediterranean region from a high resolution double nested RCM simulation. *Geophysical Research Letters*, 33(3). _eprint: https://agupubs.onlinelibrary.wiley.com/doi/pdf/10.1029/2005GL024954.

Giorgi, F. and Gutowski, W. J. (2015). Regional Dynamical Downscaling and the CORDEX Initiative. *Annual Review of Environment and Resources*, 40(1):467–490.

Gutiérrez, C., Somot, S., Nabat, P., Mallet, M., Corre, L., Meijgaard, E. V., Perpiñán, O., and Gaertner, M. A. (2020). Future evolution of surface solar radiation and photovoltaic potential in Europe: investigating the role of aerosols. *Environmental Research Letters*, 15(3):034035. Publisher: IOP Publishing.

Hawkins, E. and Sutton, R. (2009). The Potential to Narrow Uncertainty in Regional Climate Predictions. *Bulletin of the American Meteorological Society*, 90(8):1095–1107.

Herrmann, M., Somot, S., Calmanti, S., Dubois, C., and Sevault, F. (2011). Representation of spatial and temporal variability of daily wind speed and of intense wind events over the Mediterranean Sea using dynamical downscaling: impact of the regional climate model configuration. *Natural Hazards and Earth System Sciences*, 11:1983–2001. Publisher: European Geosciences Union.

Hingray, B., Blanchet, J., Evin, G., and Vidal, J.-P. (2019). Uncertainty component estimates in transient climate projections. *Climate Dynamics*.

Hingray, B. and Saïd, M. (2014). Partitioning Internal Variability and Model Uncertainty Components in a Multimember Multimodel Ensemble of Climate Projections. *Journal of Climate*, 27(17):6779–6798.

IPCC (2013). *Climate Change : The Physical Science Basis. Contribution of Working Group I to the Fifth Assessment Report of the Intergovernmental Panel on Climate Change.* [Stocker, T.F., D. Qin, G.-K. Plattner, M. Tignor, S.K. Allen, J. Boschung, A. Nauels, Y. Xia, V. Bex and P.M. Midgley (eds.)] Cambridge University Press, Cambridge, United Kingdom and New York, NY, USA. 1535 pp.

Jacob, D., Petersen, J., Eggert, B., Alias, A., Christensen, O. B., Bouwer, L. M., Braun, A., Colette, A., Déqué, M., Georgievski, G., Georgopoulou, E., Gobiet, A., Menut, L., Nikulin, G., Haensler, A., Hempelmann, N., Jones, C., Keuler, K., Kovats, S., Kröner, N., Kotlarski, S., Kriegsmann, A., Martin, E., Meijgaard, E., Moseley, C., Pfeifer, S., Preuschmann, S., Radermacher, C., Radtke, K., Rechid, D., Rounsevell, M., Samuelsson, P., Somot, S., Soussana, J.-F., Teichmann, C., Valentini, R., Vautard, R., Weber, B., and Yiou, P. (2014). EURO-CORDEX: new high-resolution climate change projections for European impact research. *Regional Environmental Change*, 14(2):563–578.

Jacob, D., Teichmann, C., Sobolowski, S., Katragkou, E., Anders, I., Belda, M., Benestad, R., Boberg, F., Buonomo, E., Cardoso, R. M., Casanueva, A., Christensen, O. B., Christensen, J. H., Coppola, E., De Cruz, L., Davin, E. L., Dobler, A., Dominguez, M., Fealy, R., Fernandez, J., Gaertner, M. A., Garcia-Diez, M., Giorgi, F., Gobiet, A., Goergen, K., Jose Gomez-Navarro, J., Gonzalez Aleman, J. J., Gutierrez, C., Gutierrez, J. M., Guttler, I., Haensler, A., Halenka, T., Jerez, S., Jimenez-Guerrero, P., Jones, R. G., Keuler, K., Kjellström, E., Knist, S., Kotlarski, S., Maraun, D., van Meijgaard, E., Mercogliano, P., Pedro Montavez, J., Navarra, A., Nikulin, G., de Noblet-Ducoudre, N., Panitz, H.-J., Pfeifer, S., Piazza, M., Pichelli, E., Pietikaeinen, J.-P., Prein, A. F., Preuschmann, S., Rechid, D., Rockel, B., Romera, R., Sanchez, E., Sieck, K., Soares, P. M. M., Somot, S., Srnec, L., Sorland, S. L., Termonia, P., Truhetz, H., Vautard, R., Warrach-Sagi, K., and Wulfmeyer, V. (2020). Regional climate downscaling over Europe : perspectives from the EURO-CORDEX community. *Regional Environmental Change*, 20(2).

Kjellström, E., Nikulin, G., Strandberg, G., Christensen, O. B., Jacob, D., Keuler, K., Lenderink, G., Meijgaard, E. v., Schär, C., Somot, S., Sørland, S. L., Teichmann, C., and Vautard, R. (2018). European climate change at global mean temperature increases of 1.5 and 2 °C above pre-industrial conditions as simulated by the EURO-CORDEX regional climate models. *Earth System Dynamics*, 9(2):459–478. Publisher: Copernicus GmbH.

Kotlarski, S., Keuler, K., Christensen, O. B., Colette, A., Déqué, M., Gobiet, A., Goergen, K., Jacob, D., Lüthi, D., van Meijgaard, E., Nikulin, G., Schär, C., Teichmann, C., Vautard, R., Warrach-Sagi, K., and Wulfmeyer, V. (2014). Regional climate modeling on European scales: a joint standard evaluation of the EURO-CORDEX RCM ensemble. *Geosci. Model Dev.*, 7(4):1297–1333.

Laux, P., Nguyen, P. N. B., Cullmann, J., Van, T. P., and Kunstmann, H. (2017). How many RCM ensemble members provide confidence in the impact of land-use land cover change? *International Journal of Climatology*, 37(4):2080–2100.

Matte, D., Larsen, M. A. D., Christensen, O. B., and Christensen, J. H. (2019). Robustness and Scalability of Regional Climate Projections Over Europe. *Frontiers in Environmental Science*, 6. Publisher: Frontiers.

McSweeney, C. F., Jones, R. G., Lee, R. W., and Rowell, D. P. (2015). Selecting CMIP5 GCMs for downscaling over multiple regions. *Climate Dynamics*, 44(11):3237–3260.

Moss, R. H., Edmonds, J. A., Hibbard, K. A., Manning, M. R., Rose, S. K., van Vuuren, D. P., Carter, T. R., Emori, S., Kainuma, M., Kram, T., Meehl, G. A., Mitchell, J. F. B., Nakicenovic, N., Riahi, K., Smith, S. J., Stouffer, R. J., Thomson, A. M., Weyant, J. P., and Wilbanks, T. J. (2010). The next generation of scenarios for climate change research and assessment. *Nature*, 463(7282):747–756.

Northrop, P. J. and Chandler, R. E. (2014). Quantifying Sources of Uncertainty in Projections of Future Climate. *Journal of Climate*, 27(23):8793–8808.

R (2017). R: A language and environment for statistical computing. https://www.r-project.org/.

Rummukainen, M. (2016). Added value in regional climate modeling. *WIREs Climate Change*, 7(1):145–159. _eprint: https://onlinelibrary.wiley.com/doi/pdf/10.1002/wcc.378.

Seneviratne, S. I., Nicholls, N., Easterling, D., Goodess, C. M., Kanae, S., Kossin, J., Luo, Y., Marengo, J., Mc Innes, K., Rahimi, M., Reichstein, M., Sorteberg, A., Vera, C., Zhang, X., Rusticucci, M., Semenov, V., Alexander, L. V., Allen, S., Benito, G., Cavazos, T., Clague, J., Conway, D., Della-Marta, P. M., Gerber, M., Gong, S., Goswami, B. N., Hemer, M., Huggel, C., Van den Hurk, B., Kharin, V. V., Kitoh, A., Klein Tank, A. M. G., Li, G., Mason, S., Mc Guire, W., Van Oldenborgh, G. J., Orlowsky, B., Smith, S., Thiaw, W., Velegrakis, A., Yiou, P., Zhang, T., Zhou, T., and Zwiers, F. W. (2012). Changes in climate extremes and their impacts on the natural physical environment. In *Managing the Risks of Extreme Events and Disasters to Advance Climate Change Adaptation*, pages 109–230. Cambridge University Press. Num Pages: 122.

Sørland, S. L., Schär, C., Lüthi, D., and Kjellström, E. (2018). Bias patterns and climate change signals in GCM-RCM model chains. *Environmental Research Letters*, 13(7):074017. Publisher: IOP Publishing.

Stroeve, J. C., Kattsov, V., Barrett, A., Serreze, M., Pavlova, T., Holland, M., and Meier, W. N. (2012). Trends in Arctic sea ice extent from CMIP5, CMIP3 and observations. *Geophysical Research Letters*, 39(16). _eprint: https://agupubs.onlinelibrary.wiley.com/doi/pdf/10.1029/2012GL052676.

Taylor, K. E., Stouffer, R. J., and Meehl, G. A. (2011). An Overview of CMIP5 and the Experiment Design. *Bulletin of the American Meteorological Society*, 93(4):485–498.

Tramblay, Y. and Somot, S. (2018). Future evolution of extreme precipitation in the Mediterranean. *Climatic Change*.

Vautard, R., Kadygrov, N., Iles, C., Boberg, F., Buonomo, E., Bülow, K., Coppola, E., Corre, L., Meijgaard, E. v., Nogherotto, R., Sandstad, M., Schwingshackl, C., Somot, S., Aalbers, E., Christensen, O. B., Ciarlò, J. M., Demory, M.-E., Giorgi, F., Jacob, D., Jones, R. G., Keuler, K., Kjellström, E., Lenderink, G., Levavasseur, G., Nikulin, G., Sillmann, J., Solidoro, C., Sørland, S. L., Steger, C., Teichmann, C., Warrach-Sagi, K., and Wulfmeyer, V. (2020). Evaluation of the large EURO-CORDEX regional climate model ensemble. *Journal of Geophysical Research: Atmospheres*, n/a(n/a):e2019JD032344. _eprint: https://agupubs.onlinelibrary.wiley.com/doi/pdf/10.1029/2019JD032344.

von Storch, H. and Zwiers, F. (2013). Testing ensembles of climate change scenarios for "statistical significance". *Climatic Change*, 117(1):1–9.

Yip, S., Ferro, C. A. T., Stephenson, D. B., and Hawkins, E. (2011). A Simple, Coherent Framework for Partitioning Uncertainty in Climate Predictions. *Journal of Climate*, 24(17):4634–4643.

Zappa, G. and Shepherd, T. G. (2017). Storylines of Atmospheric Circulation Change for European Regional Climate Impact Assessment. *Journal of Climate*, 30(16):6561–6577. Publisher: American Meteorological Society.